REFERENCES

[1] Porphyrin [online]. Available from: http://en.wikipedia.org/wiki/Porphyrin [2007, January 5]

[2] Wasielewski, M. R. Photoinduced Electron Transfer in Supramolecular Systems for Artificial Photosynthesis. *Chem. Rev.* **1992**, *92*, 435-461.

[3] Zheng, J.; Konishi, K.; Aida, T. Guest-Selective Binding of Z-Amino Acids by a Strapped Metalloporphyrin Receptor with a Hydrogen-Bonding Capability. *Tetrahedron* **1997**, *53*, 9115-9122.

[4] Collman, J. P.; Wagenknecht, P. S.; Hutchison, J. E. Molecular Catalysts for Multielectron Redox Reactions of Small Molecules: The "Cofacial Metallodiporphyrin" Approach. *Angew. Chem., Int. Ed. Engl.* **1994**, *33*, 1537-1554.

[5] Gust, D. Very Small Arrays. *Nature* **1997**, *386*, 21-22.

[6] Vicente, M. G. H.; Shetty, S.; Wickramasinghe, A.; Smith, K. M. Syntheses of Carbon-Carbon Linked Carboranylated Porphyrins for Application in Boron Neutron Capture Therapy of Cancer. *Tetrahedron Lett.* **2000**, *41*, 7623-7627.

[7] Kenner, G. W.; McCombie, S. W.; Smith, K. M. J. *Chem. Soc., Perkin Trans 1.* **1973**, *21*, 2517.

[8] Smith, K.M.; Unsworth, J.F. The Nuclear Magnetic Resonance Spectra of Porphyrins-IX. Carbon-13 NMR Spectra of Some Chlorins and Other Chlorophyll Degradation Products. *Tetrahedron* **1975**, *31*, 367–375.

[9] Abraham, R. J.; Medforth,C. J.; Smith, K. M.; Goff, D. A.; Simpson, D. J. NMR Spectra of Porphyrins. Part 31. Ring Currents in Hydroporphyrins. *J. Am. Chem. Soc.* **1987**, *109*, 4786-4791.

[10] (a) Rothemund, P. Formation of Porphyrins from Pyrrole and Aldehydes. *J. Am. Chem. Soc.* **1935**, *57*, 2010-2011. (b) Rothemund, P.; Menotti, A. R. Porphyrin Studies. IV. The Synthesis of α,β,γ,δ-Tetraphenylporphine. *J. Am. Chem. Soc.* **1941**, *63*, 267-270.

[11] Rothemund, P. A New Porphyrin Synthesis. The Synthesis of Porphin. *J. Am. Chem. Soc.* **1936**, *58*, 625-627.

[12] Rothemund, P. Porphyrin Studies. III. The Structure of the Porphine Ring System. *J. Am. Chem. Soc.* **1939**, *61*, 2912-2915.

[13] Adler, A. D.; Longo, F. R.; Finarelli, J. D.; Goldmacher, J.; Assour, J.; Korsakoff, L. A Simplified Synthesis for *meso*-Tetraphenylporphine. *J. Org. Chem.* **1967**, *32*, 476.

[14] Lindsey, J. S.; Schreiman, I. C.; Hsu, H. C.; Kearney, P. C.; Marguerettaz, A. M. Rothemund and Adler-Longo Reactions Revisited: Synthesis of Tetraphenyl Porphyrins under Equilibrium Conditions. *J. Org. Chem.* **1987**, *52*, 827-836.

[15] Sessler, J. L.; Mozaffari, A; Johnson, M. R. *Org. Synth.* **1991**, *70*, 68.

[16] Whitlock, H. W.; Hanauer, Jr. R. Octaethylporphyrin. *J. Org. Chem.* **1968**, *33*, 2169-2171.

[17] Arsenault, G. P.; Bullock, E.; MacDonald, S. F. Pyrromethanes and Porphyrins Therefrom. *J. Am. Chem. Soc.* **1960**, *82*, 4384-4389.

[18] Sessler, J. L.; Cyr, M. J.; Lynch, V.; McGhee, E.; Ibers, J. A. Synthetic and Structural Studies of Sapphyrin, a 22-.pi.-Electron Pentapyrrolic "Expanded Porphyrin". *J. Am. Chem. Soc.* **1990**, *112*, 2810-2813.

[19] Furuta, H.; Asano, T.; Ogawa, T. "N-Confused Porphyrin": A New Isomer of Tetraphenylporphyrin. *J. Am. Chem. Soc.* **1994**, *116*, 767-768.

[20] Reimers, J. R.; Lü, T. X.; Crossley, M. J.; Hush, N. S. The Mechanism of Inner-Hydrogen Migration in Free Base Porphyrin: *Ab Initio* MP2 Calculations. *J. Am. Chem. Soc.* **1995**, *117*, 2855-2861.

[21] Naruta, Y.; Tani, F.; Maruyama, K. *meso*-Perfluorination of Porphyrins with *N*-fluoropyridinium Triflate. *Tetrahedron Lett.* **1992**, *33*, 1069-1072.

[22] (a) Chorghade, M. S.; Dolphin, D.; Dupré D.; Hill, D. R.; Lee, E. C.; Wijesekera, T. P. *Synthesis* **1996**, 1320-1324. (b) Ali, H.; van Lier, J. E. Phenylselenyl Halides: Efficient Reagents for The Selective Halogenation and Nitration of Porphyrins. *Tetrahedron Lett.* **1991**, *32*, 5015-5018.

[23] (a) Jaquinod, L.; Khoury, R. G.; Shea, K. M.; Smith, K. M. Regioselective Syntheses and Structural Characterizations of 2,3-Dibromo-and 2,3,7,8,12,13-Hexabromo-5,10,15,20-Tetraphenylporphyrins. *Tetrahedron* **1999**, *55*, 13151-13158. (b) Crossley, M. J.; Harding, M. M.;

Sternhell, S. Tautomerism in 2-Substituted 5,10,15,20-Tetraphenyl porphyrins. *J. Am. Chem. Soc.* **1986**, *108*, 3608-3613.

[24] Boyle R. W.; Jonhson C. K.; Dolphin, D. Iodination and Heck Alkynylation of 5,15-Diphenylporphyrin. A Convenient Entry to Asymmetrically *meso*-Substituted Porphyrins. *J. Chem. Soc., Chem. Commun.* **1995**, 527-528.

[25] (a) Shea, K. M.; Jaquinod, L.; Smith, K. M. Dihydroporphyrin Synthesis: New Methodology. *J. Org. Chem.* **1998**, *63*, 7013-7021. (b) Baldwin, J. E.; Crossley, M. J.; DeBernardis, J. Efficient Peripheral Functionalization of Porphyrins. *Tetrahedron* **1982**, *38*, 685-692.

[26] (a) Smith, K. M.; Lai, J. J. Syntheses of Heme d Models. *J. Am. Chem. Soc.* **1984**, *106*, 5746-5748. (b) Vasudevan, J.; Stibrany, R. T.; Bumby, J.; Knapp, S.; Potenza, J. A.; Emge, T. J.; Schugar, H. J. An Edge-Over-Edge Zn(II) Bacteriochlorin Dimer Having an Unshifted Q_y Band. The Importance of π-Overlap. *J. Am. Chem. Soc.* **1996**, *118*, 11676-11677. (c) Stolzenberg, A. M.; Simerly, S. W.; Steffey, B. D.; Haymond, G. S. The Synthesis, Properties, and Reactivities of Free-Base and Zn(II)-*N*-Methyl Hydroporphyrin Compounds. The Unexpected Selectivity of the Direct Methylation of Free-Base Hydroporphyrin Compounds. *J. Am. Chem. Soc.* **1997**, *119*, 11843-11854.

[27] (a) Fuhrhop, J. H.; Besecke, S.; Subramanian, J.; Mengersen, Chr.; Riesner, D. Reactions of Oxophlorines and Their .pi. Radicals. *J. Am. Chem. Soc.* **1975**, *97*, 7141-7152. (b) Chang, C. K.; Sotiriou, C. C-Hydroxy- and C-methylchlorins. A Convenient Route to Heme d and Bonellin Model Compounds. *J. Org. Chem.* **1985**, *50*, 4989-4991.

[28] Adler, A. D.; Longo, F. R.; Kampas, F.; Kim, J. On The Preparation of Metalloporphyrins. *J. Inorg. Nucl. Chem.* **1970**, *2*, 2443-2445.

[29] Gosztola, D.; Niemczyk, M. P.; Wasielewski, M. R. Picosecond Molecular Switch Based on Bidirectional Inhibition of Photoinduced Electron Transfer Using Photogenerated Electric Fields. *J. Am. Chem. Soc.* **1998**, *120*, 5118-5119.

[30] Wagner, R. W.; Lindsey, J. S.; Seth, J.; Palaniappan, V.; Bocian, D. F. Molecular Optoelectronic Gates. *J. Am. Chem. Soc.* **1996**, *118*, 3996-3997.

[31] De Silva, A. P.; Gunaratne, H. Q. N.; Gunnlaugsson, T.; Huxley, A. J. M.; McCoy, C. P.; Rademacher, J. T.; Rice, T. E. Signaling Recognition Events with Fluorescent Sensors and Switches. *Chem. Rev.* **1997**, *97*, 1515-1566.

[32] Wagner, R. W.; Lindsey, J. S. A Molecular Photonic Wire. *J. Am. Chem. Soc.* **1994**, *116*, 9759-9760.

[33] Jasat, A.; Dolphin, D. Expanded Porphyrins and Their Heterologs. *Chem. Rev.* **1997**, *97*, 2267-2340.

[34] (a) Kumble, R.; Palese, S.; Lin, V. S.-Y.; Therien, M. J.; Hochstrasser, R. M. Ultrafast Dynamics of Highly Conjugated Porphyrin Arrays. *J. Am. Chem. Soc.* **1998**, *120*, 11489-11498. (b) Strachan, J.-P.; Gentemann, S.; Seth, J.; Kalsbeck, W. A.; Lindsey, J. S.; Holten, D.; Bocian, D. F. Synthesis and Characterization of Tetrachlorodiarylethyne-Linked Porphyrin Dimers. Effects of Linker Architecture on Intradimer Electronic Communication. *Inorg. Chem.* **1998**, *37*, 1191-1201.

[35] H. Tamiaki. Supramolecular Structure in Extramembraneous Antennae of Green Photosynthetic Bacteria. *Coord. Chem. Rev.* **1996**, *148*, 183-197.

[36] Bhyrappa, P.; Wilson, S. R.; Suslick, K. S. Hydrogen-Bonded Porphyrinic Solids: Supramolecular Networks of Octahydroxy Porphyrins. *J. Am. Chem. Soc.* **1997**, *119*, 8492-8502.

[37] Endisch, C.; Fuhrhop, J.-H.; Buschmann, J.; Luger, P.; Siggel, U. β-Tetraethyl-β'-tetrapyridin-4-yl Porphyrins, Their *N*-Methylated Tetracations, and Heterodimers with *ms*-Tetraphenylsulfonato Porphyrins. *J. Am. Chem. Soc.* **1996**, *118*, 6671-6680.

[38] Wojaczynski, J.; Latos-Grazynski, L. Monomeric and Trimeric Manganese(III) Complexes of 2-Hydroxy-5,10,15,20-tetraphenylporphyrin. Synthesis and Characterization. *Inorg. Chem.* **1996**, *35*, 4812-4818.

[39] Fleischer, E. B.; Shachter, A. M. Coordination Oligomers and a Coordination Polymer of Zinc Tetraarylporphyrins. *Inorg. Chem.* **1991**, *30*, 3763-3769.

[40] Anderson, S.; Anderson, H. L.; Sanders, J. K. M. Expanding Roles for Templates in Synthesis. *Acc. Chem. Res.* **1993**, *26*, 469-475.

[41] Anderson, S.; Anderson, H. L.; Bashall, A.; McPartlin, M.; Sanders, J.K.M.

Assembly and Crystal Structure of A Photoactive Array of Five Porphyrins. *Angew. Chem., Int. Ed. Engl.* **1995**, *34*, 1096-1099.

[42] Chernook, A. V.; Rempel, U.; von Borczyskowski, C.; Shulga, A. M.; Zenkevich, E. I. Formation and Optical Properties of Self-Organized Pentameric Porphyrin Arrays. *Chem. Phys. Lett.* **1996**, *254*, 229-241.

[43] Funatsu, K.; Kimura, A.; Imamura, T.; Ichimura, A.; Sasaki, Y. Perpendicularly Arranged Ruthenium Porphyrin Dimers and Trimers *Inorg. Chem.* **1997**, *36*, 1625-1635.

[44] Funatsu, K.; Imamura, T.; Ichimura, A.; Sasaki, Y. Synthesis and Properties of Cyclic Ruthenium(II) Porphyrin Tetramers. *Inorg. Chem.* **1998**, *37*, 1798-1804.

[45] Kariya, N.; Imamura,; T.; Sasaki, Y. Synthesis, Characterization, and Spectral Properties of New Perpendicularly Linked Osmium(II) Porphyrin Oligomers. *Inorg. Chem.* **1997**, *36*, 833-839.

[46] Drain, C. M.; Lehn J. M. Self-assembly of Square Multiporphyrin Arrays by Metal Ion Coordination. *J. Chem. Soc., Chem. Commun.* **1994**, 2313-2315.

[47] Yuan, H.; Thomas, L.; Woo, L. K. Synthesis and Characterization of Mono-, Bis-, and Tetrakis-Pyridyltriarylporphyrin Pd(II) and Pt(II) Supramolecular Assemblies. Molecular Structure of a Pd-Linked Bisporphyrin Complex. *Inorg. Chem.* **1996**, *35*, 2808-2817.

[48] Kurtikyan, T. S.; Mardyukov, A. N.; Goodwin, J. A. Interaction of Nitrogen Oxides with Sublimed Layers of (*meso*-Tetraphenylporphyrinato) cobalt(II); IR Evidence of Oxo-Transfer from (Nitro)porphyrinatocobalt (III) to Free Nitric Oxide. *Inorg. Chem.* **2003**, *42*, 8489-8493.

[49] Nakagawa, K.; Kumon, K.; Tsutsumi, C.; Tabuchi, K.; Kitagawa, T.; Sadaoka, Y. HCl Gas Sensing Properties of $TPPH_2$ Dispersed in Varios Copolymers. *Sens. Actuat. B.* **2000**, *65*, 138-140.

[50] Smith, V. C.; Batty, S. V.; Richardson, T.; Foster, K. A.; Johnstone, R. A. W.; Sobral, A. J. F. N.; Rocha Gonsalves, A. M.'A. Chlorine Sensing Properties of Porphyrin Thin Films. *Thin Solid Films* **1996**, *284-285*, 911-914.

[51] D'Amico, A.; Natale, C. D.; Paolesse, R.; Macagnano, A.; Mantini, A.

Metalloporphyrins as Basic Material for Volatile Sensitive Sensors. *Sens. Actuat. B.* **2000**, *65*, 209-215.

[52] CzolkSens, R. Studies on The Anion Sensitivity of Immobilized Metalloporphyrins for Application as Optochemical Sensors. *Sens. Actuat. B.* **1996**, *30*, 61-63.

[53] Natale, C. D.; Salimbeni, D.; Paolesse, R.; Macagnano, A.; D'Amico, A. Porphyrins-based Opto-Electronic Nose for Volatile Compounds Detection. *Sens. Actuat. B.* **2000**, *65*, 220-226.

[54] Umar, A. A.; Salleh, M. M.; Yahaya, M. Self-Assembled Monolayer of Copper(II) meso-Ttetra(4-sulfanatophenyl)porphyrin as an Optical Gas Sensor. *Sens. Actuat B.* **2004**, *101*, 231-235.

[55] Spadavecchia, J.; Rella, R.; Siciliano, P.; Manera, M.G.; Alimelli, A.; Paolesse, R.; Di Natale, C.; D'Amico, A. Optochemical Vapour Detection Using Spin Coated Thin Film of ZnTPP. *Sens. Actuat B.* **2006**, *115*, 12-16.

[56] Alessio, E.; Macchi, M.; Heath, S. L.; Marzilli, L. G. Ordered Supramolecular Porphyrin Arrays from a Building Block Approach Utilizing Pyridylporphyrins and Peripheral Ruthenium Complexes and Identification of a New Type of Mixed-Metal Building Block. *Inorg. Chem.* **1997**, *36*, 5614-5623.

APPENDICES

APPENDIX A

Spectroscopic Data

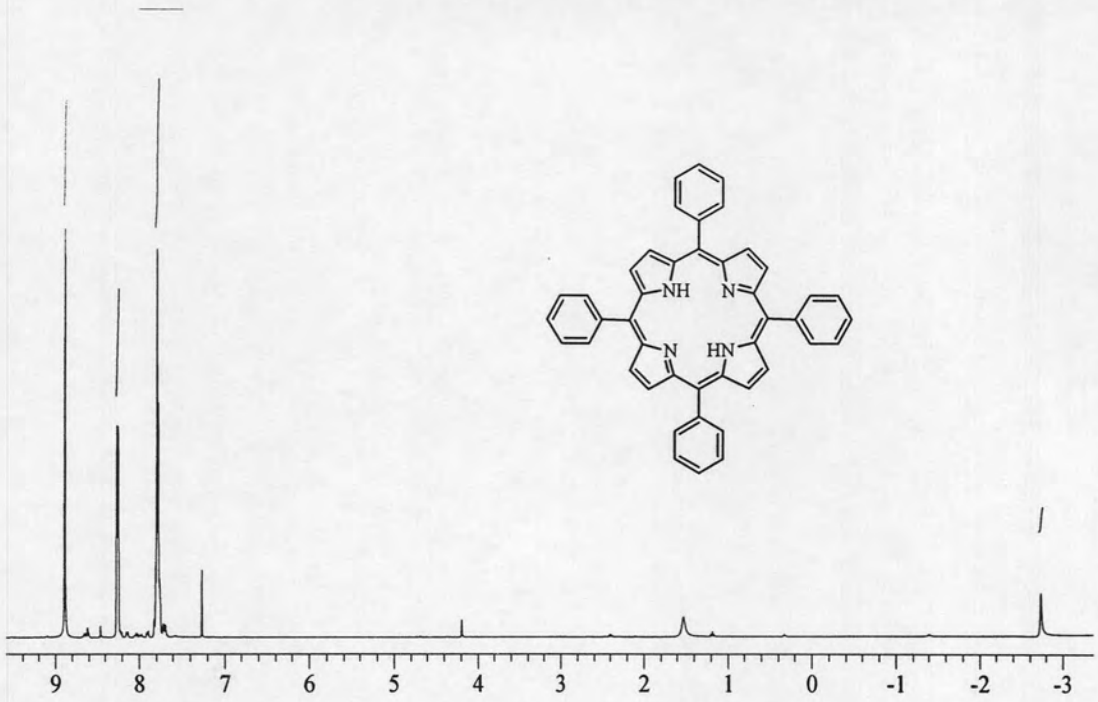

Figure A-1 The ^{1}H NMR spectrum of 5,10,15,20-tetraphenylporphyrin (TPP, **1**)

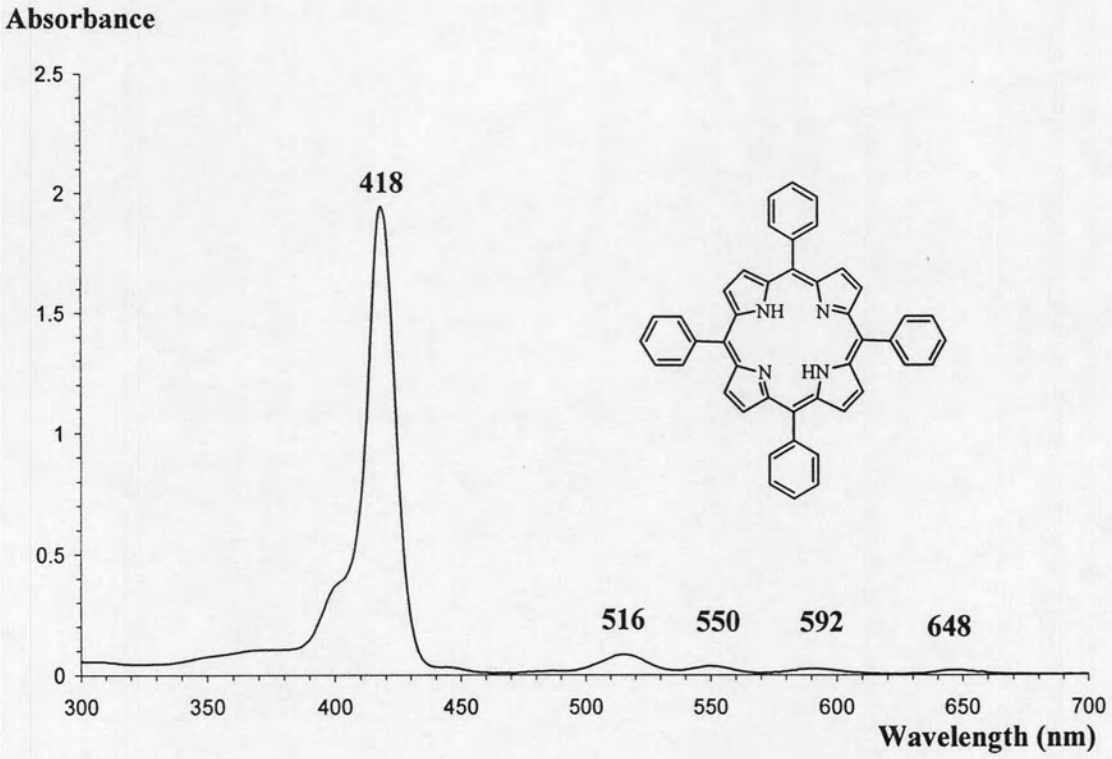

Figure A-2 UV/Visible spectrum of 5,10,15,20-tetraphenylporphyrin (TPP, **1**)

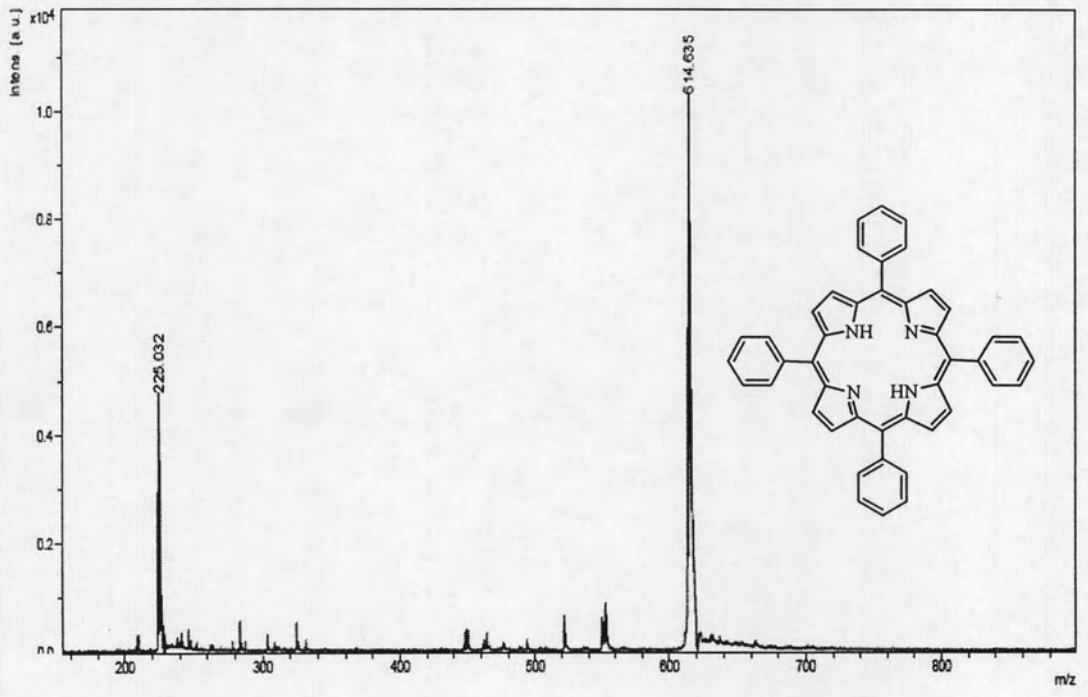

Figure A-3 MALDI-TOF mass spectrum of 5,10,15,20-tetraphenylporphyrin (TPP, **1**)

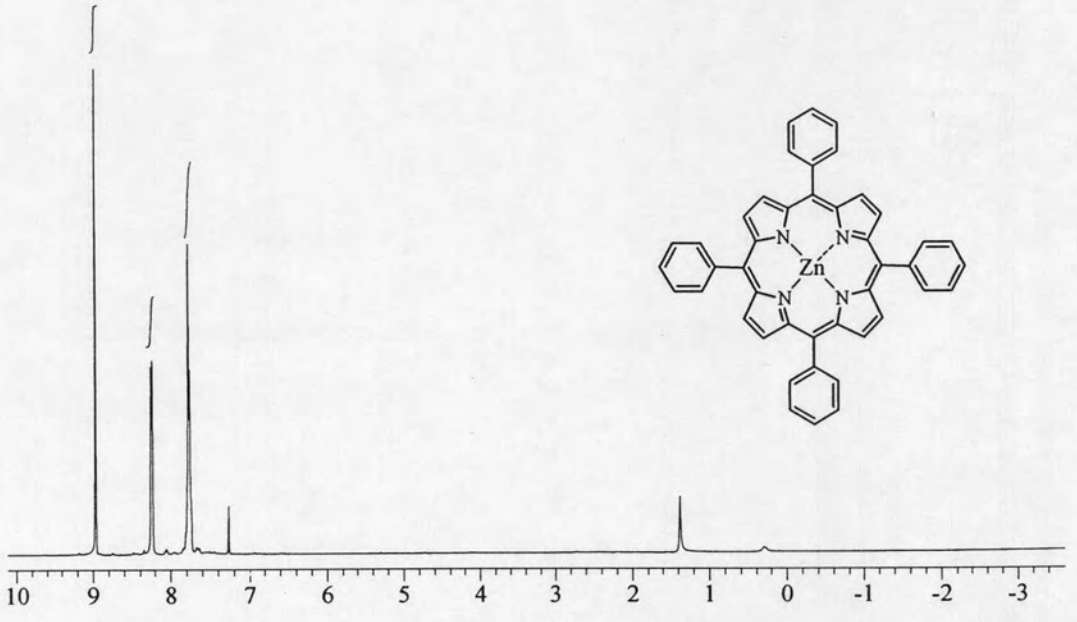

Figure A-4 The ^{1}H NMR spectrum of 5,10,15,20-tetraphenyl porphyrinatozinc(II) (ZnTPP, **2**)

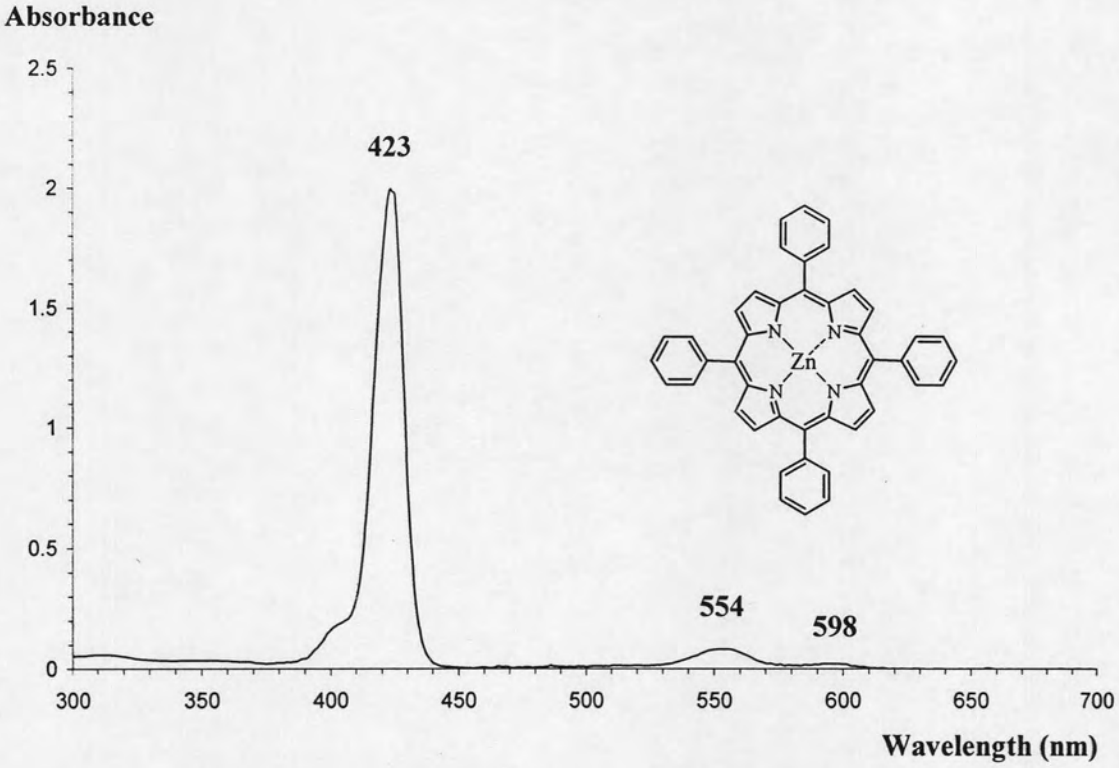

Figure A-5 UV/Visible spectrum of 5,10,15,20-tetraphenylporphyrinatozinc(II) (ZnTPP, **2**)

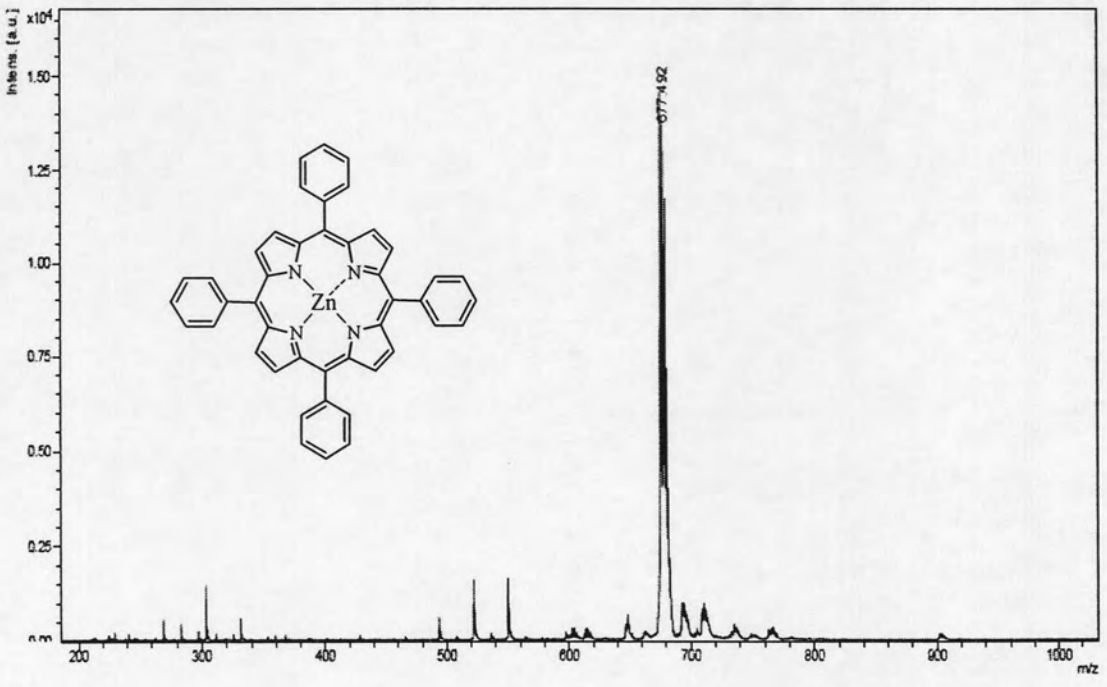

Figure A-6 MALDI-TOF mass spectrum of 5,10,15,20-tetraphenyl porphyrinatozinc(II) (ZnTPP, **2**)

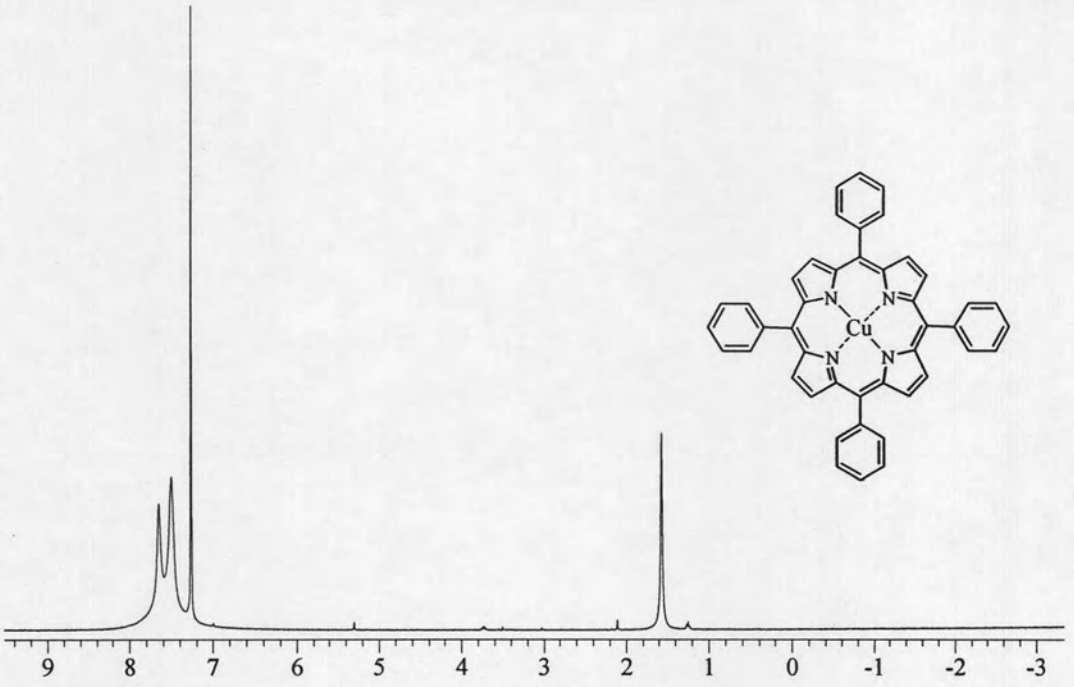

Figure A-7 The ^{1}H NMR spectrum of 5,10,15,20-tetraphenylporphyrinatocopper(II) (CuTPP, **3**)

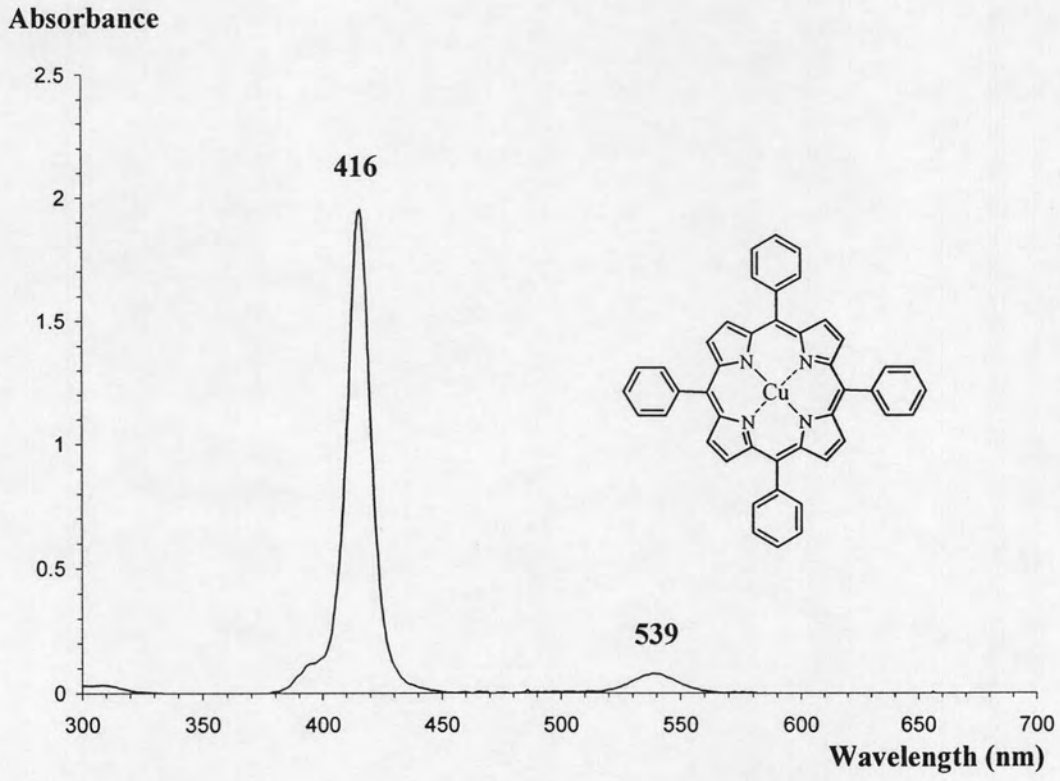

Figure A-8 UV/Visible spectrum of 5,10,15,20-tetraphenylporphyrinatocopper(II) (CuTPP, **3**)

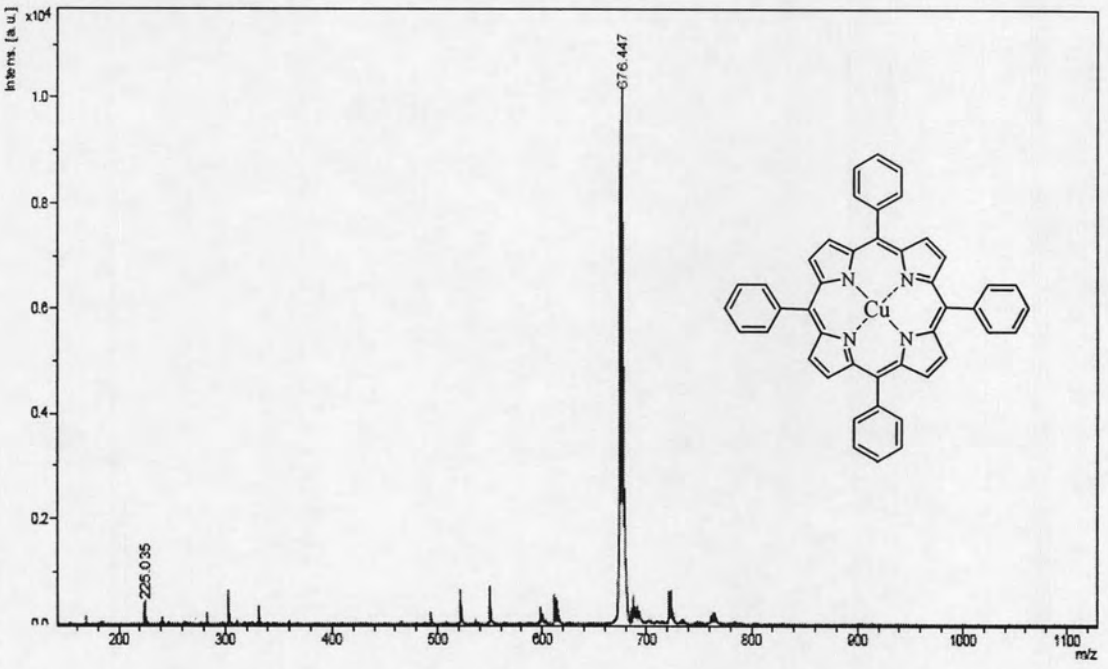

Figure A-9 MALDI-TOF mass spectrum of 5,10,15,20-tetraphenyl porphyrinatocopper(II) (CuTPP, **3**)

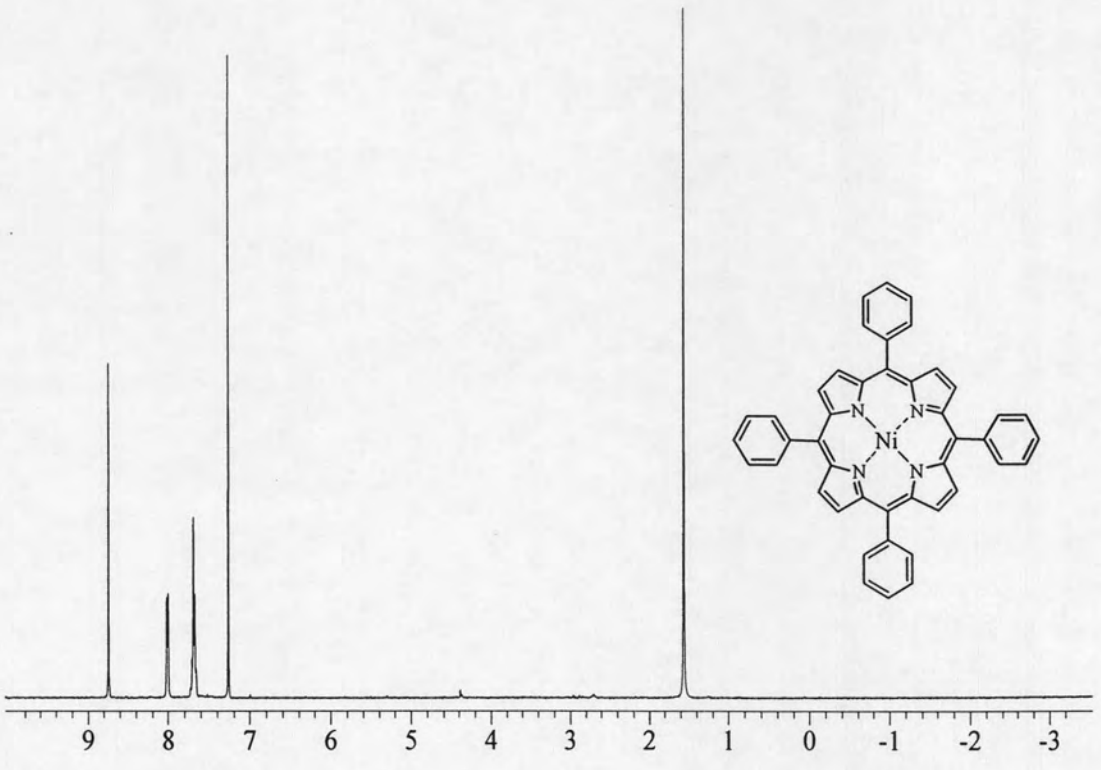

Figure A-10 The ^{1}H NMR spectrum of 5,10,15,20-tetraphenyl porphyrinatonickel(II) (NiTPP, **4**)

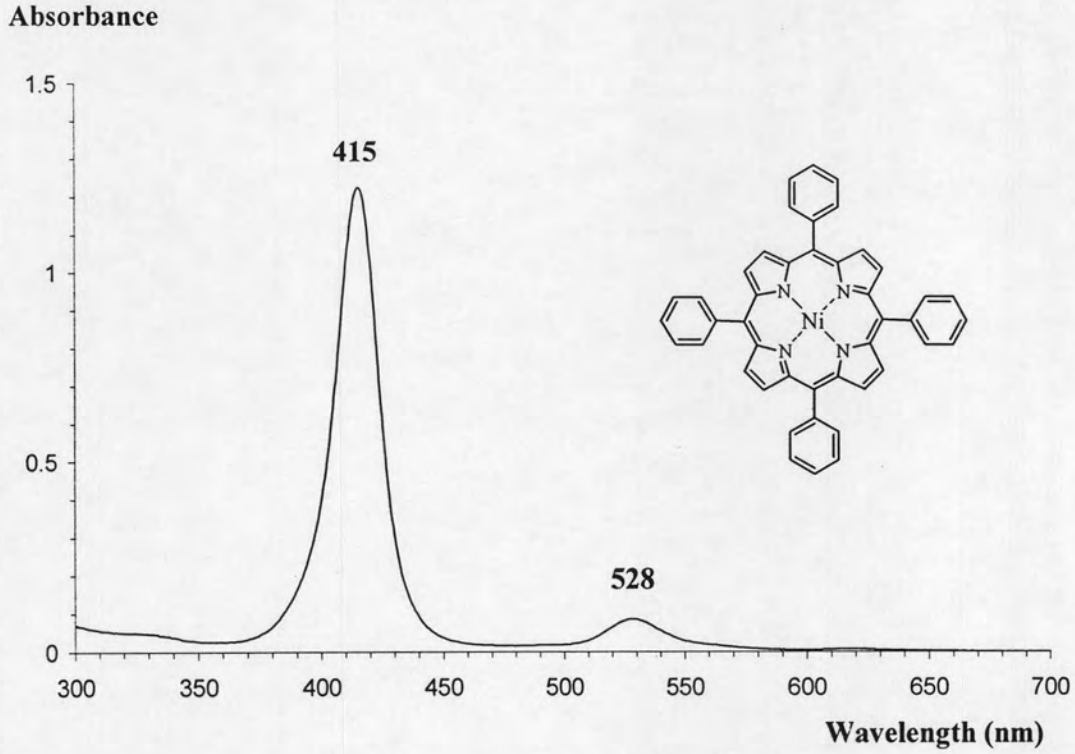

Figure A-11 UV/Visible spectrum of 5,10,15,20-tetraphenylporphyrinatonickel(II) (NiTPP, **4**)

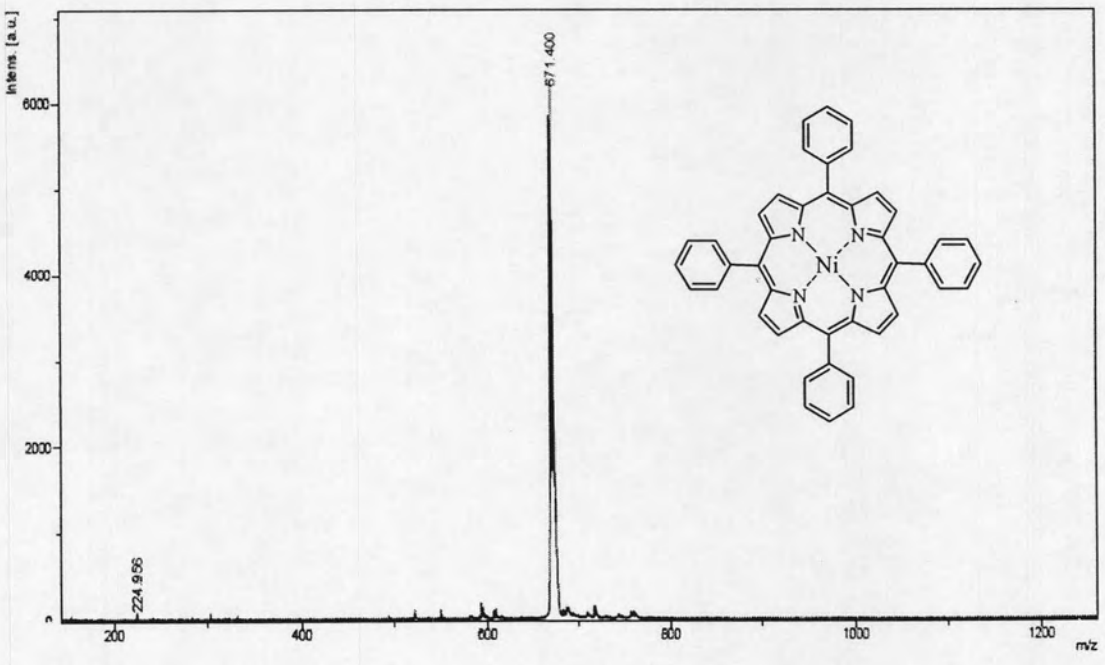

Figure A-12 MALDI-TOF mass spectrum of 5,10,15,20-tetraphenyl porphyrinatonickel(II) (NiTPP, **4**)

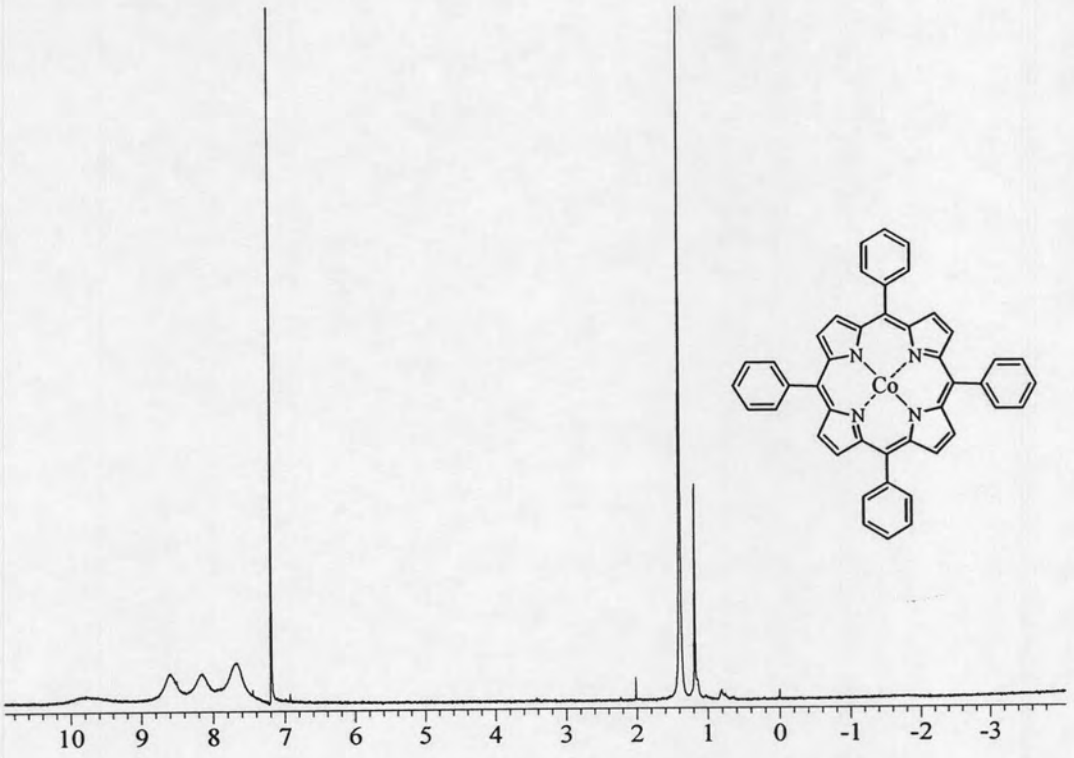

Figure A-13 The ^{1}H NMR spectrum of 5,10,15,20-tetraphenyl porphyrinatocobalt(II) (CoTPP, **5**)

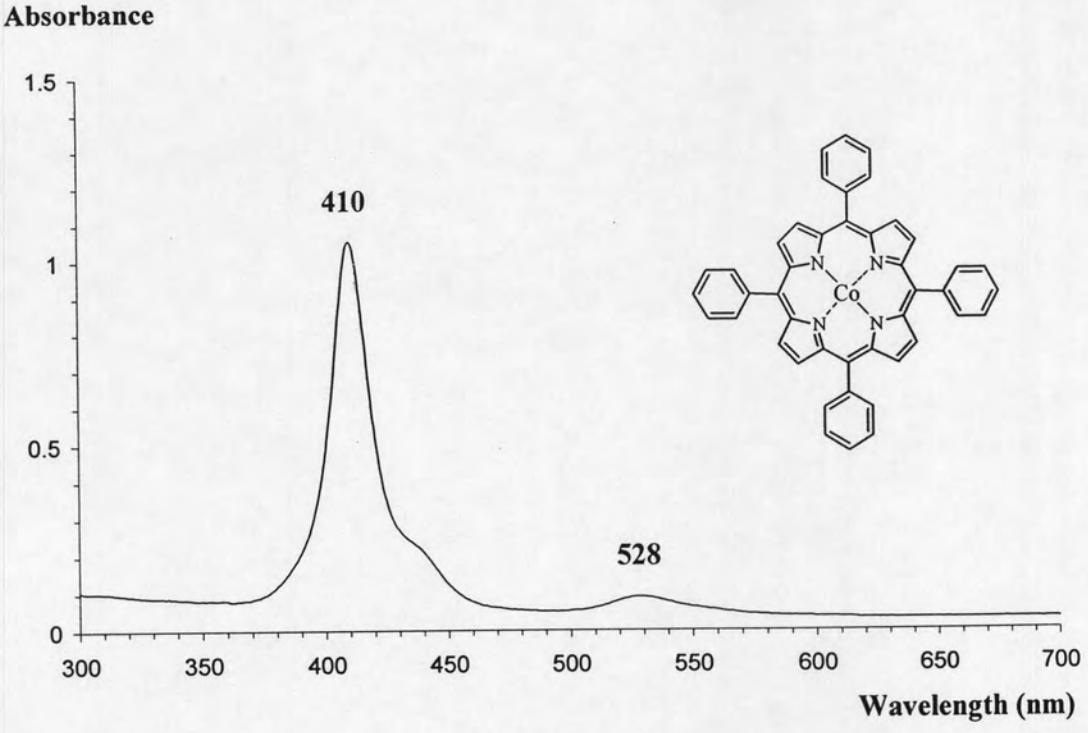

Figure A-14 UV/Visible spectrum of 5,10,15,20-tetraphenylporphyrinatocobalt(II) (CoTPP, **5**)

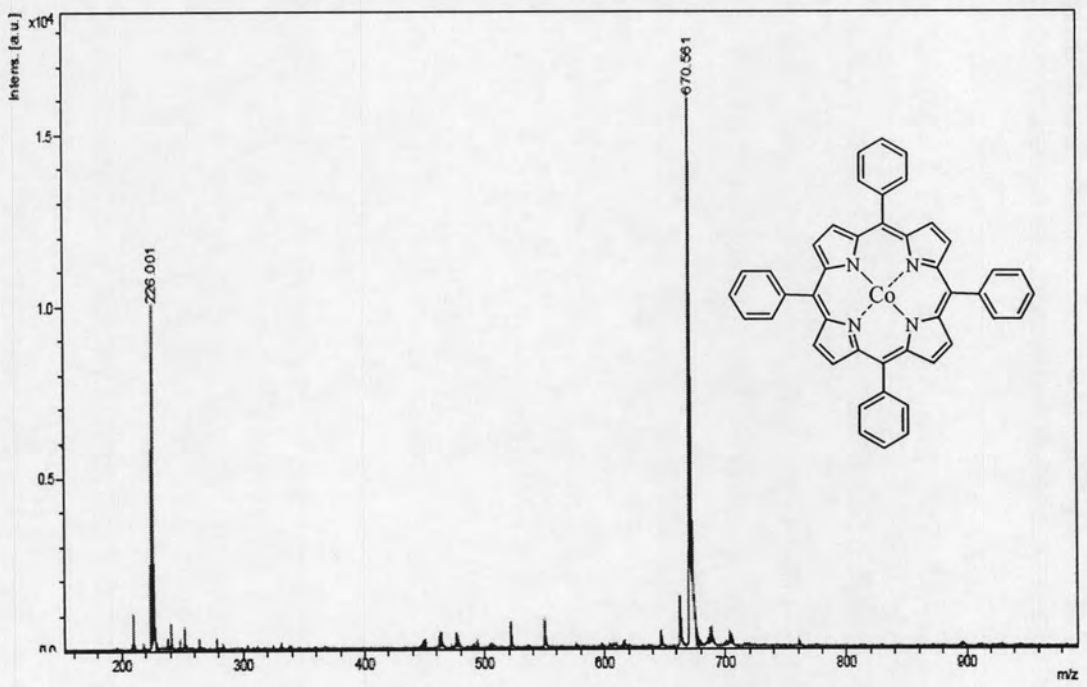

Figure A-15 MALDI-TOF mass spectrum of 5,10,15,20-tetraphenyl porphyrinatocobalt(II) (CoTPP, **5**)

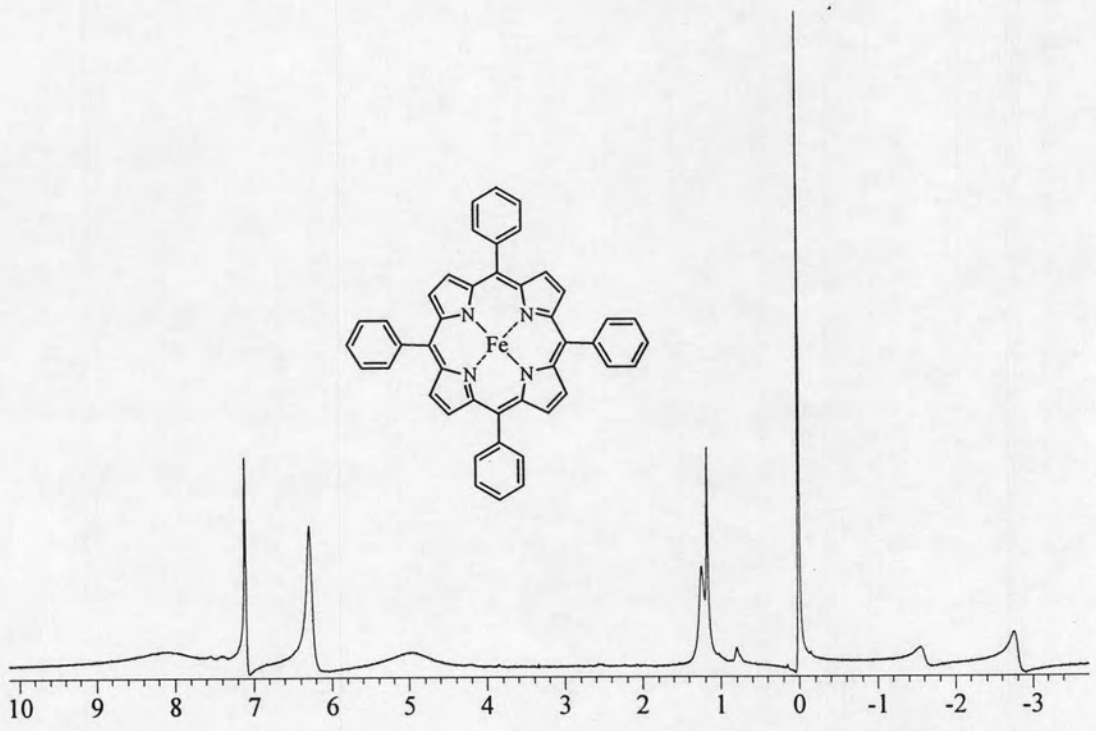

Figure A-16 The ^{1}H NMR spectrum of 5,10,15,20-tetraphenylporphyrinatoiron(III) ((Cl)FeTPP, **6**)

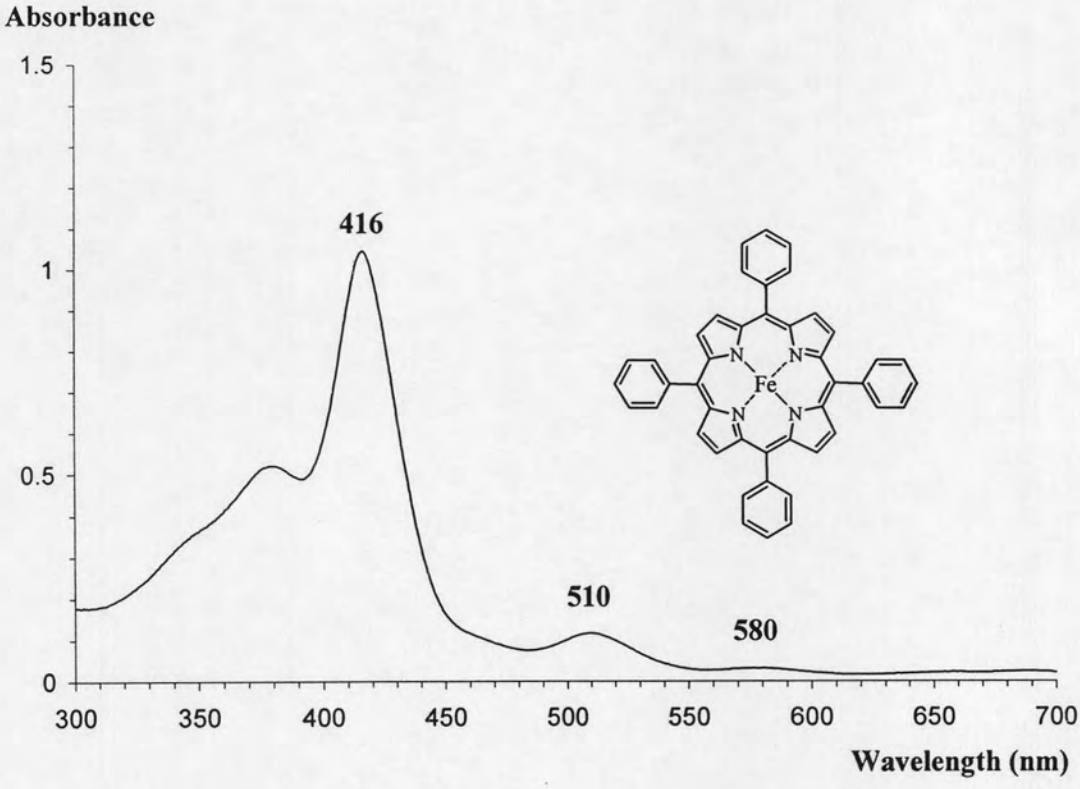

Figure A-17 UV/Visible spectrum of 5,10,15,20-tetraphenylporphyrinatoiron(III) ((Cl)FeTPP, **6**)

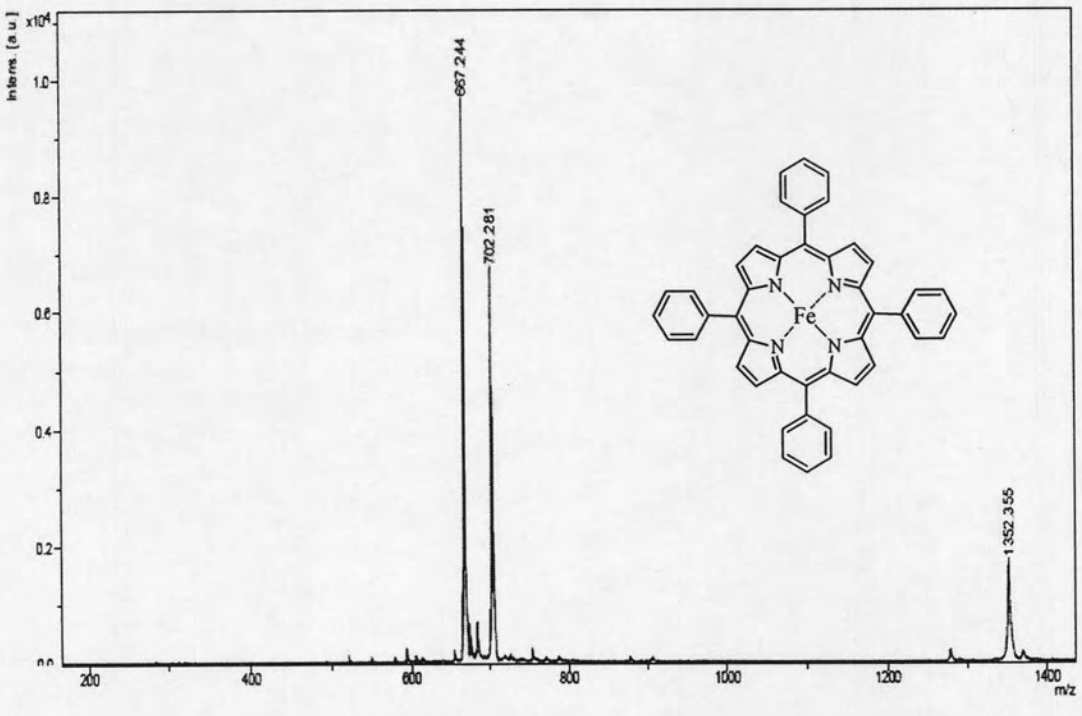

Figure A-18 MALDI-TOF mass spectrum of 5,10,15,20-tetraphenyl porphyrinatoiron(III) ((Cl)FeTPP, **6**)

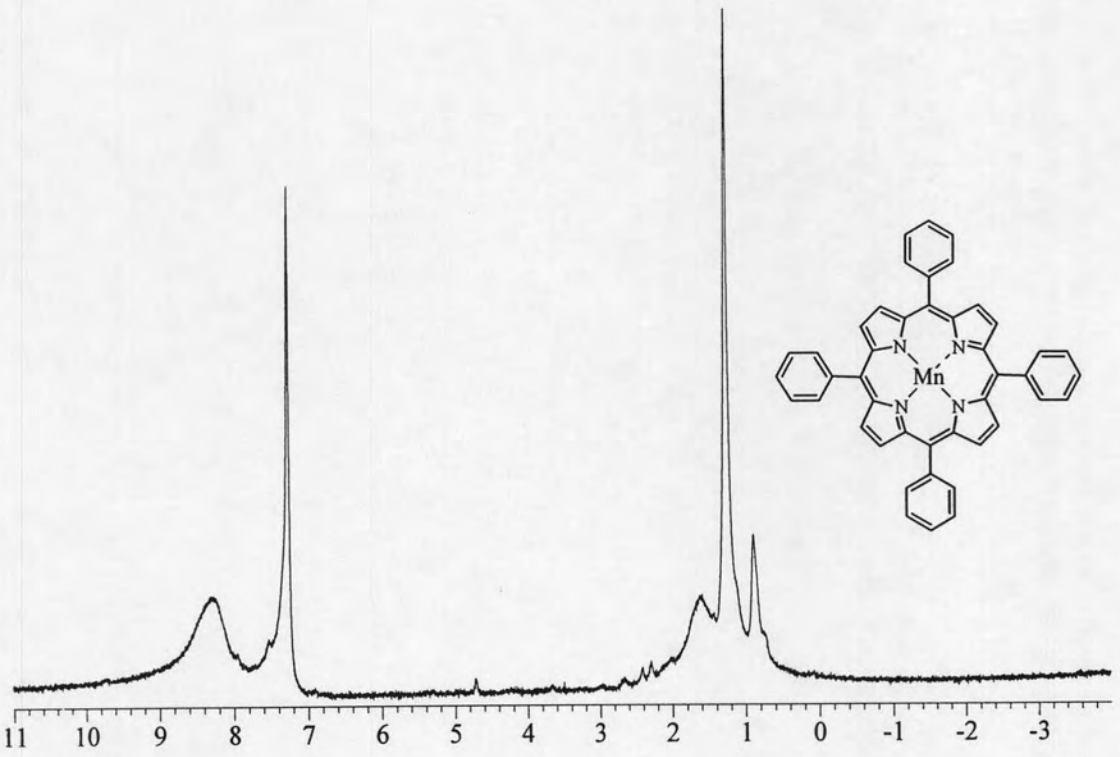

Figure A-19 The ^{1}H NMR spectrum of 5,10,15,20-tetraphenyl porphyrinatomanganese(III) (MnTPP, **7**)

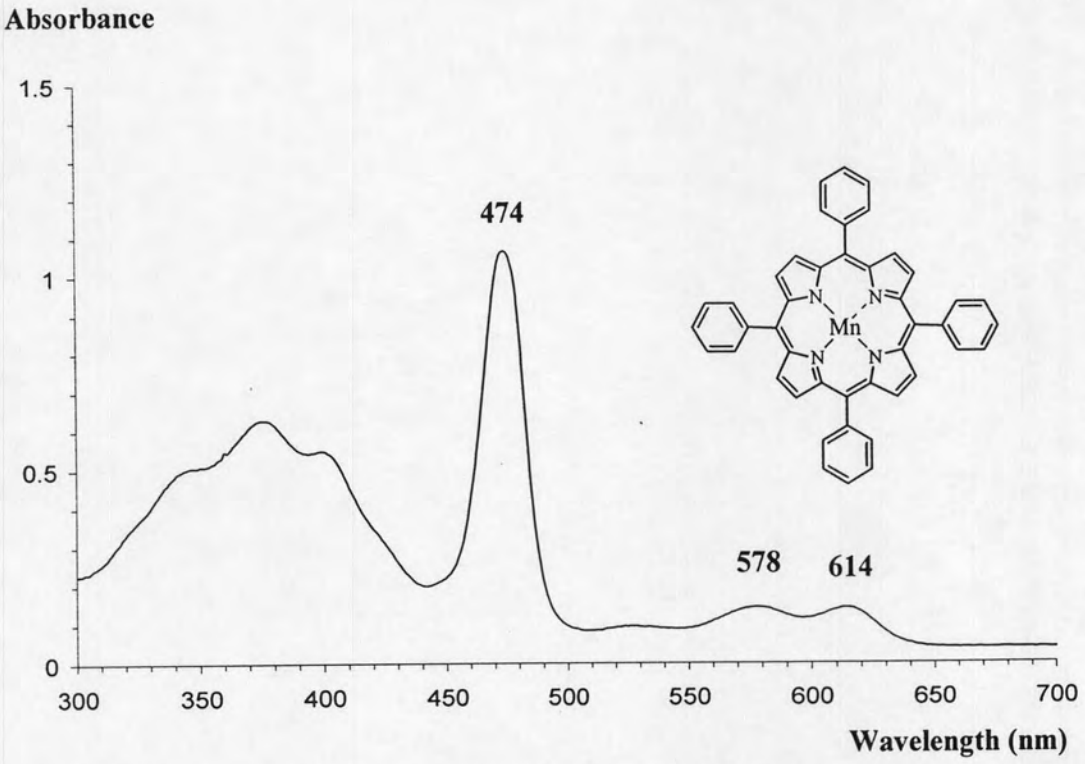

Figure A-20 UV/Visible spectrum of 5,10,15,20-tetraphenylporphyrinato manganese(III) (MnTPP, **7**)

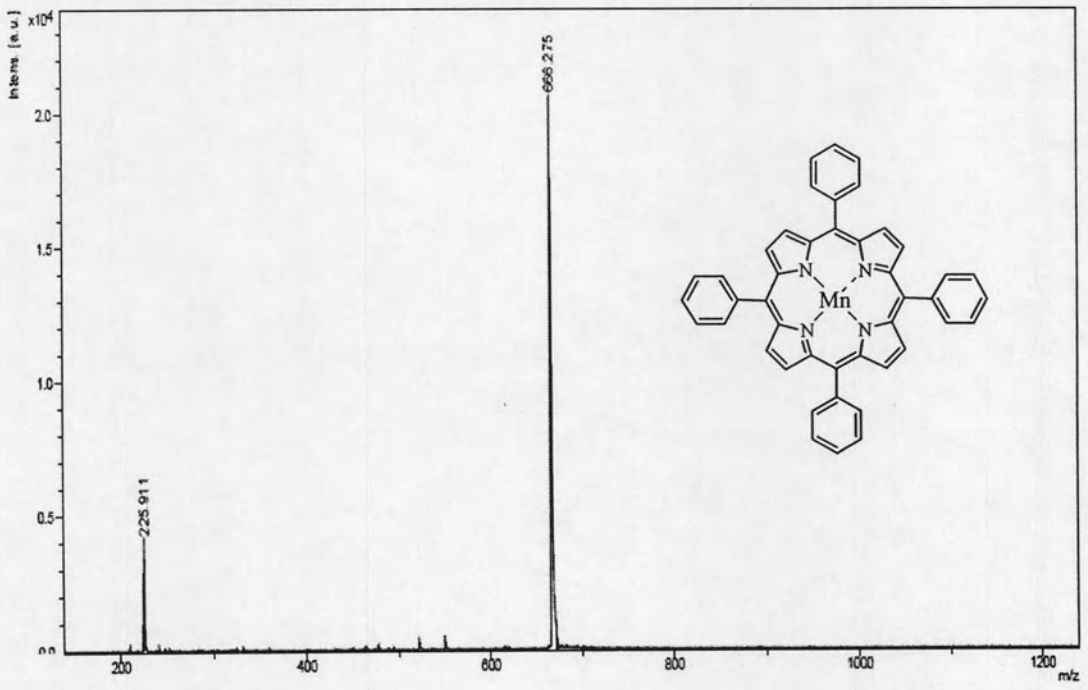

Figure A-21 MALDI-TOF mass spectrum of 5,10,15,20-tetraphenylporphyrinato manganese(III) (MnTPP, **7**)

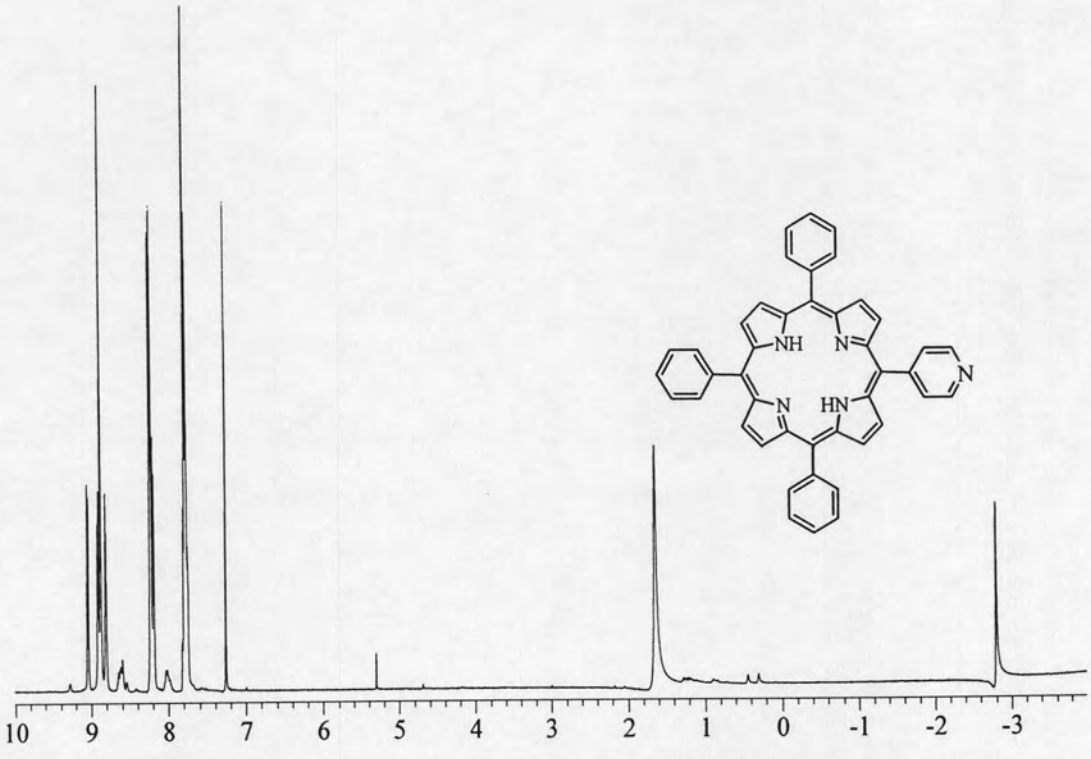

Figure A-22 The ^{1}H NMR spectrum of 5-(pyridyl)-10,15,20-triphenylporphyrin (MPyTPP, **8**)

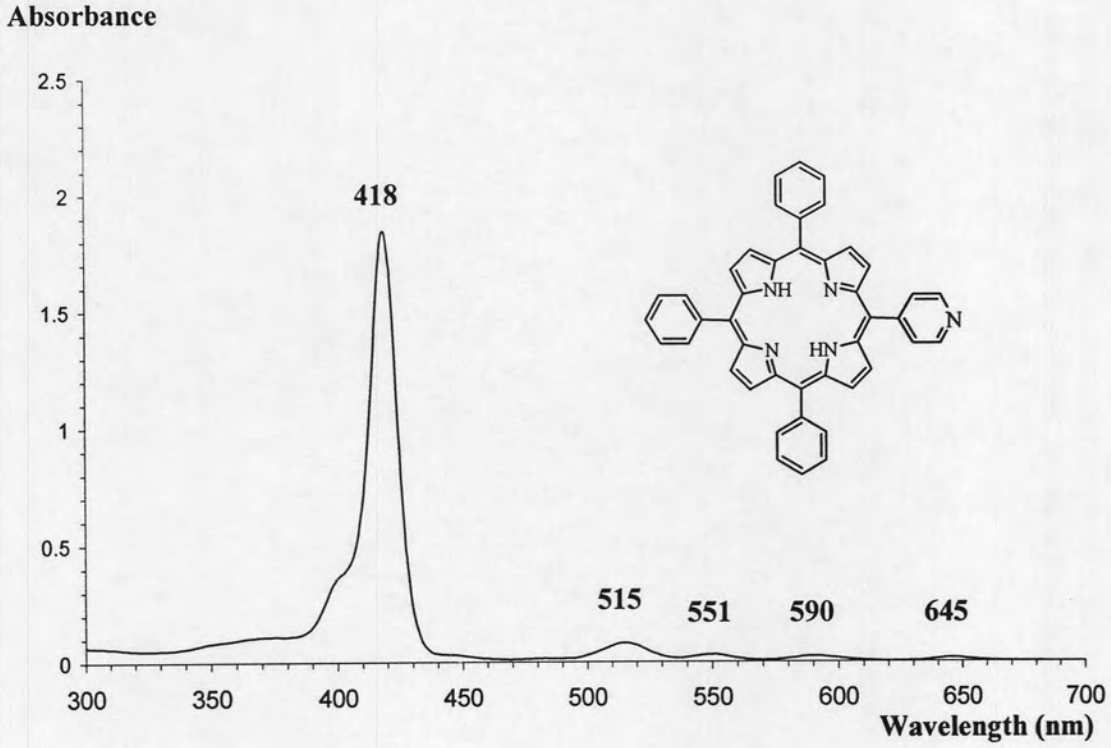

Figure A-23 UV/Visible spectrum of 5-(pyridyl)-10,15,20-triphenylporphyrin (MPyTPP, **8**)

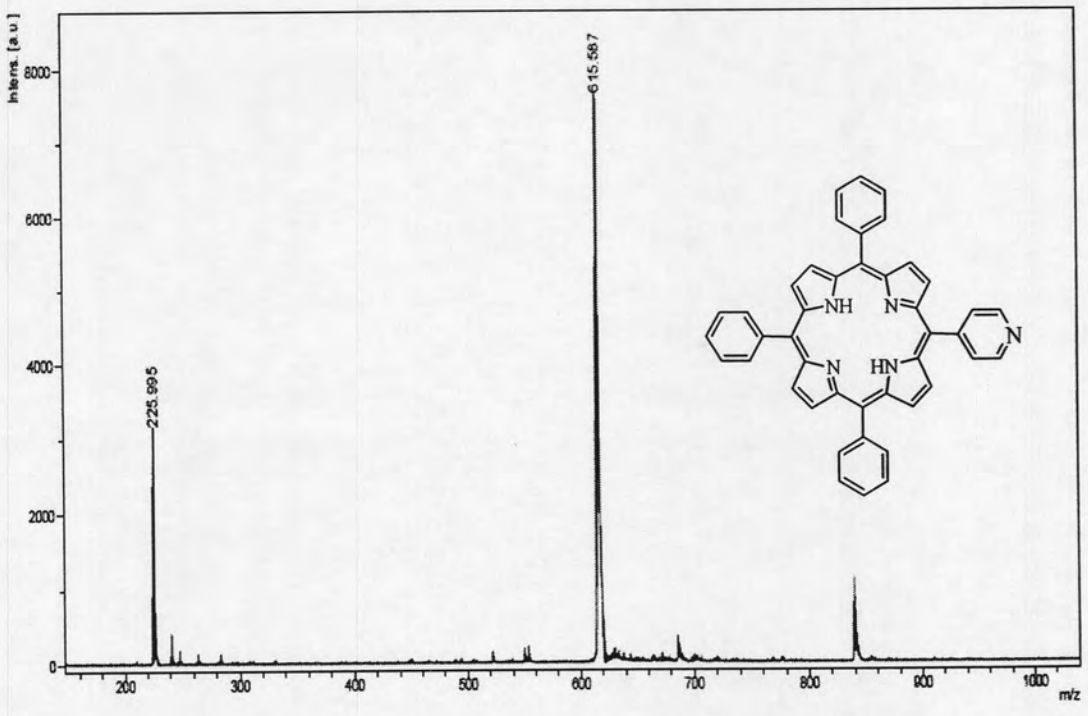

Figure A-24 MALDI-TOF mass spectrum of 5-(pyridyl)-10,15,20-triphenyl porphyrin (MPyTPP, **8**)

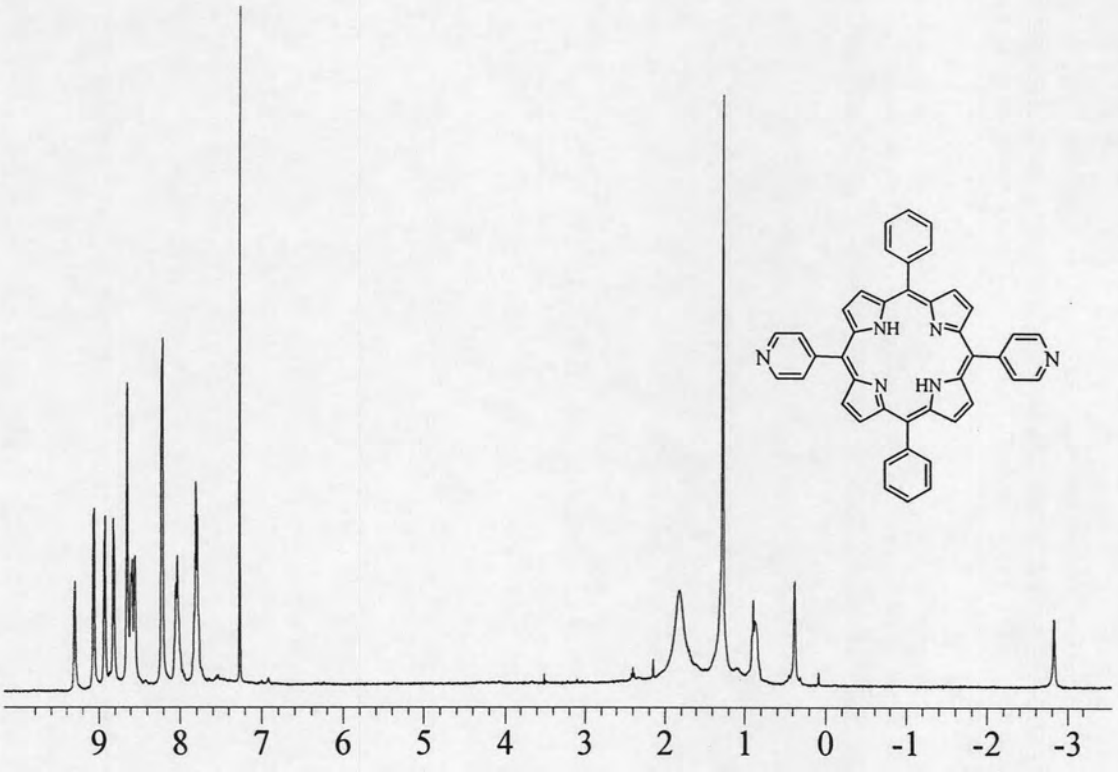

Figure A-25 The ^{1}H NMR spectrum of 5,15-(dipyridyl)-10,20-diphenylporphyrin (*trans*-DPyDPP, **9**)

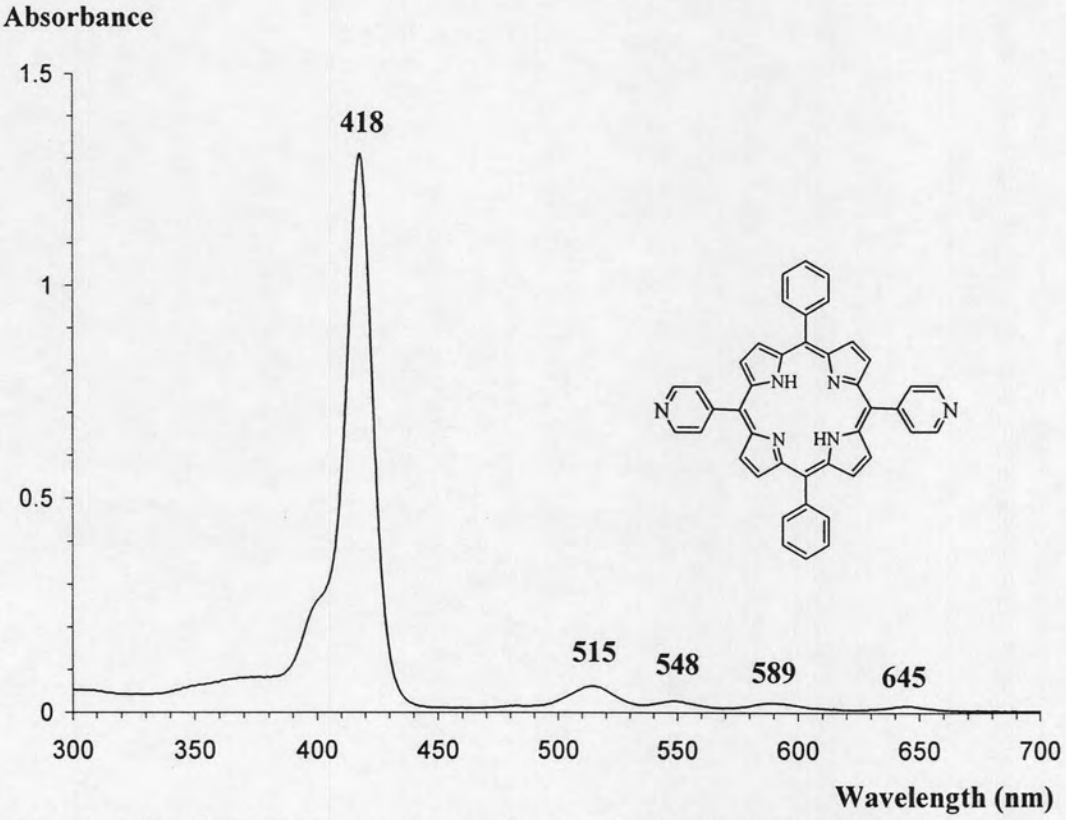

Figure A-26 UV/Visible spectrum of 5,15-(dipyridyl)-10,20-diphenylporphyrin (*trans*-DPyDPP, **9**)

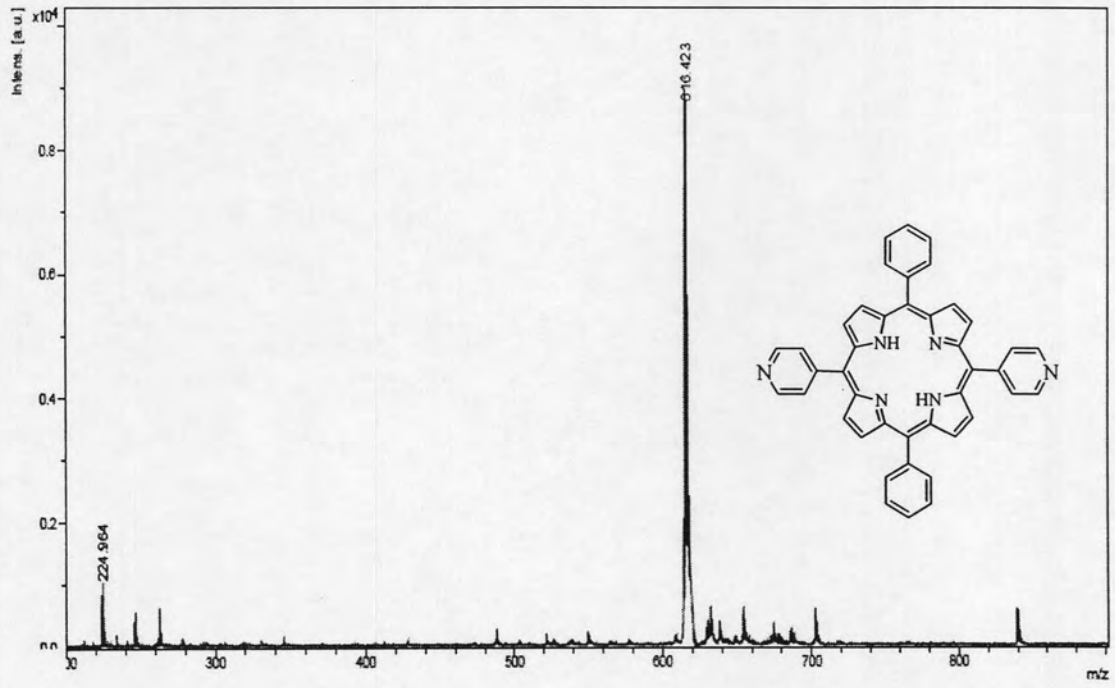

Figure A-27 MALDI-TOF mass spectrum of 5,15-(dipyridyl)-10,20-diphenyl porphyrin (*trans*-DPyDPP, **9**)

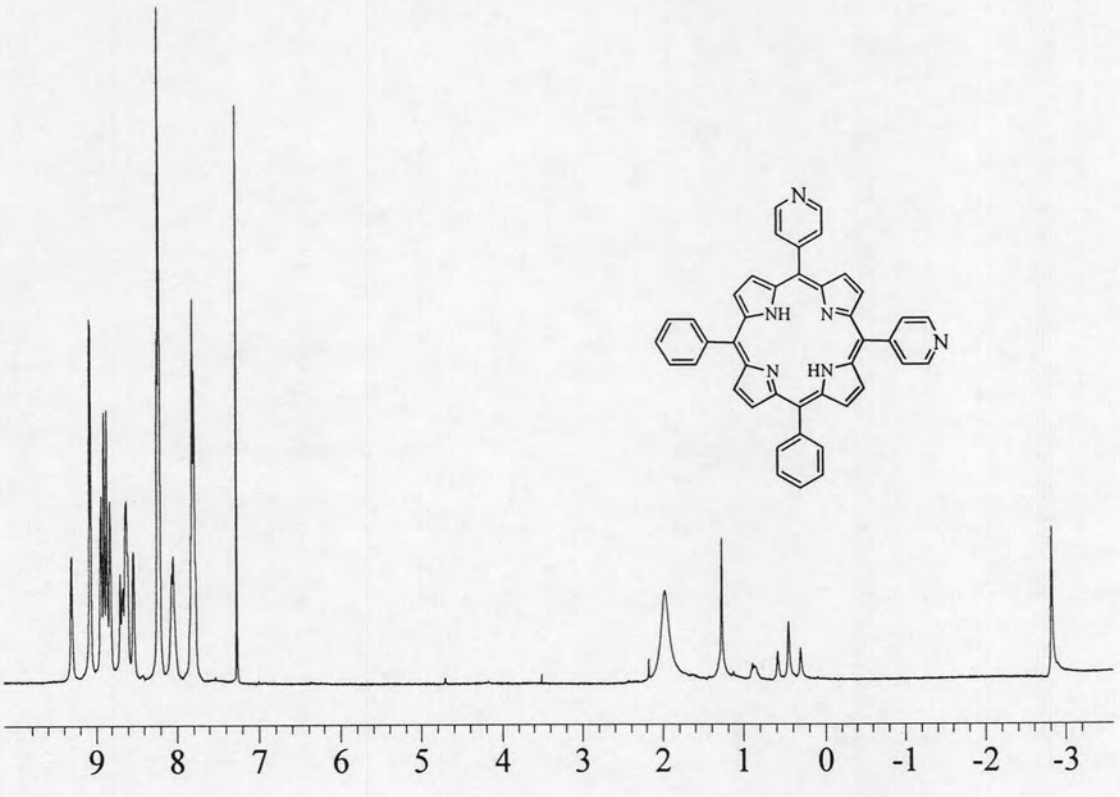

Figure A-28 The ^{1}H NMR spectrum of 5,10-(dipyridyl)-15,20-diphenylporphyrin (*cis*-DPyDPP, **10**)

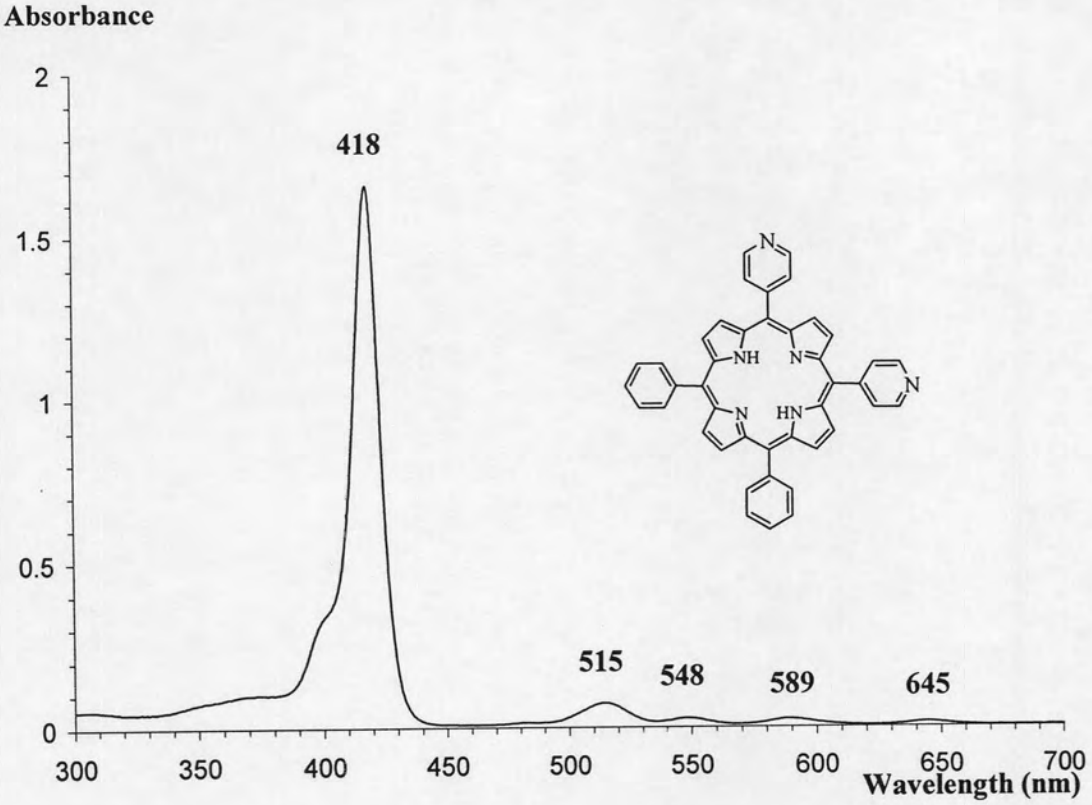

Figure A-29 UV/Visible spectrum of 5,10-(dipyridyl)-15,20-diphenylporphyrin (*cis*-DPyDPP, **10**)

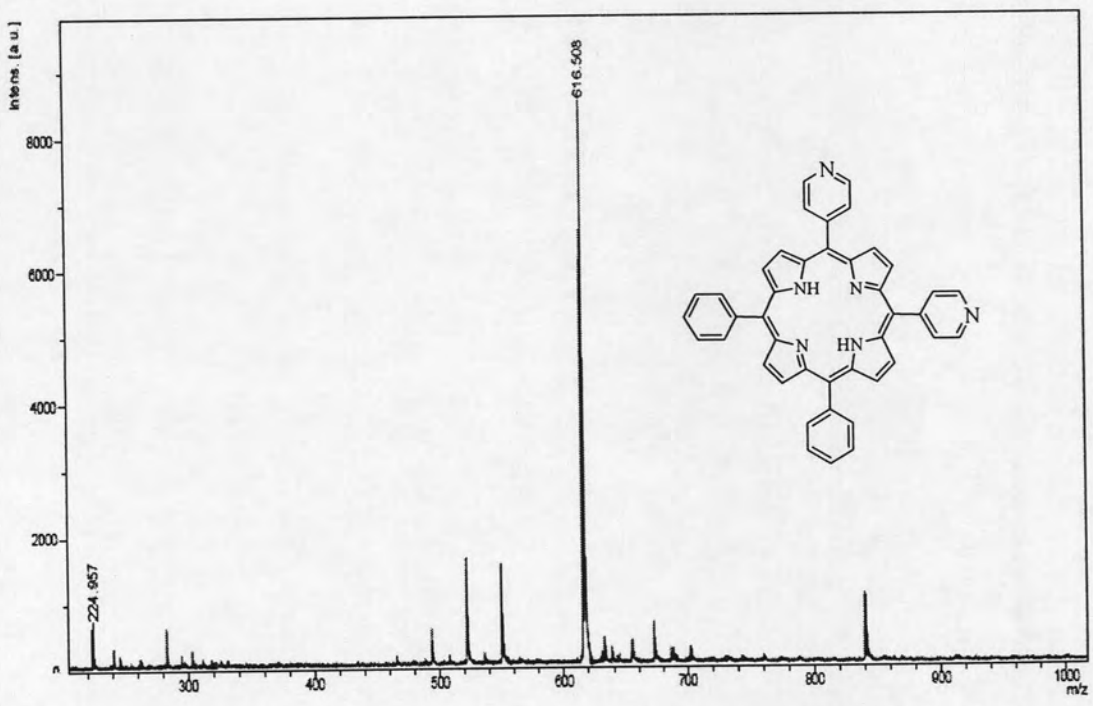

Figure A-30 MALDI-TOF mass spectrum of 5,10-(dipyridyl)-15,20-diphenyl porphyrin (*cis*-DPyDPP, **10**)

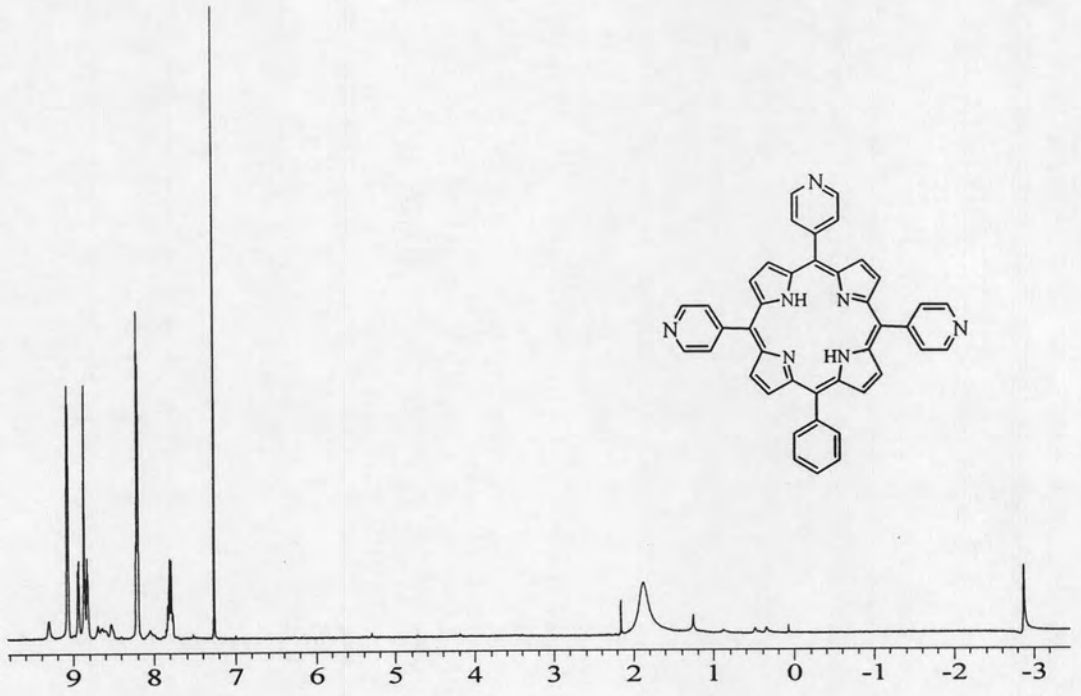

Figure A-31 The ^{1}H NMR spectrum of 5,10,15-(tripyridyl)-20-phenylporphyrin (TPyMPP, **11**)

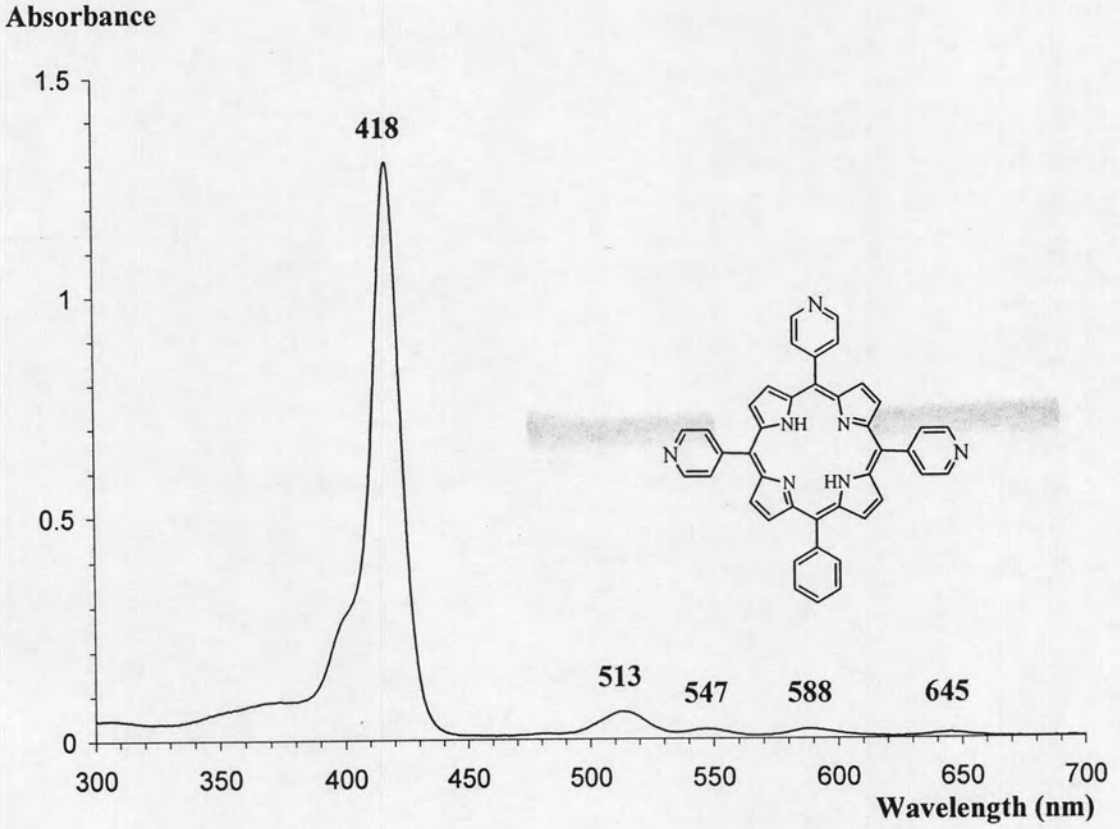

Figure A-32 UV/Visible spectrum of 5,10,15-(tripyridyl)-20-phenylporphyrin (TPyMPP, **11**)

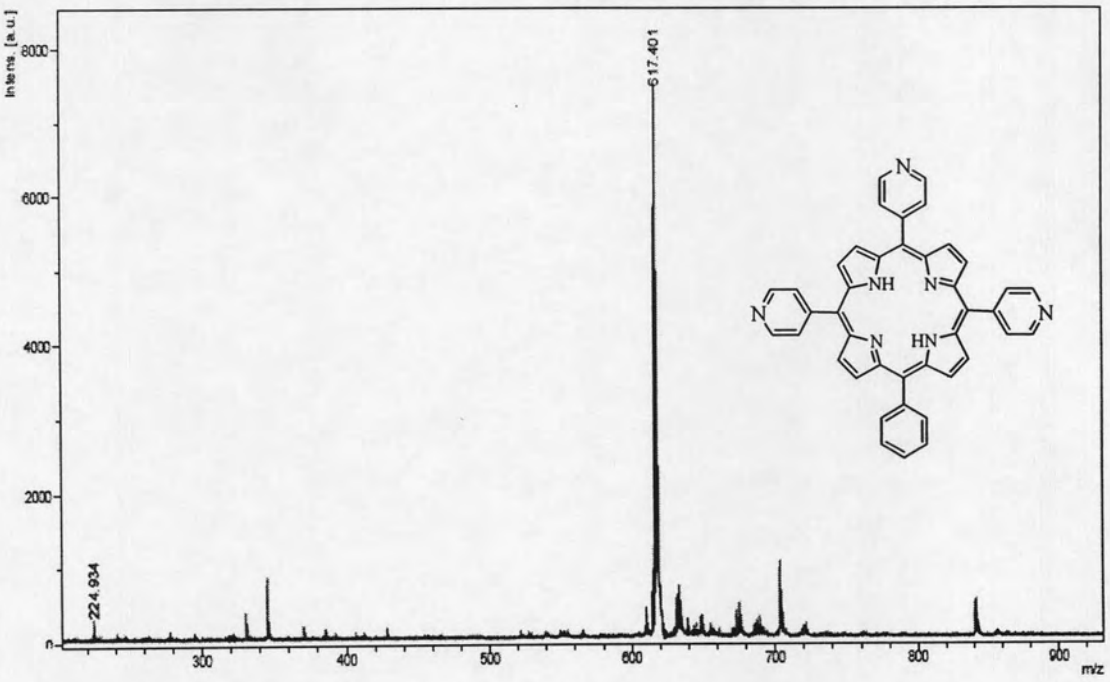

Figure A-33 MALDI-TOF mass spectrum of 5,10,15-(tripyridyl)-20-phenyl porphyrin (TPyMPP, **11**)

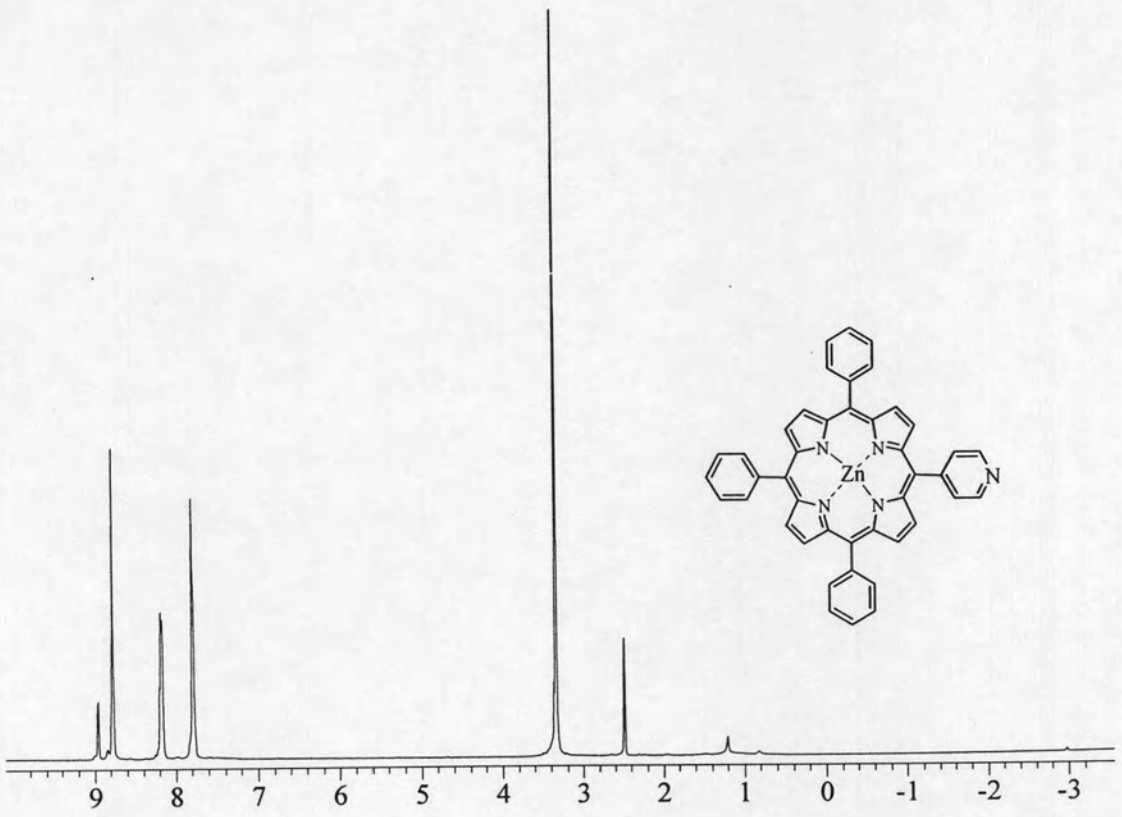

Figure A-34 The ^{1}H NMR spectrum of 5-(pyridyl)-10,15,20-triphenyl porphyrinatozinc(II) (ZnMPyTPP, **12**)

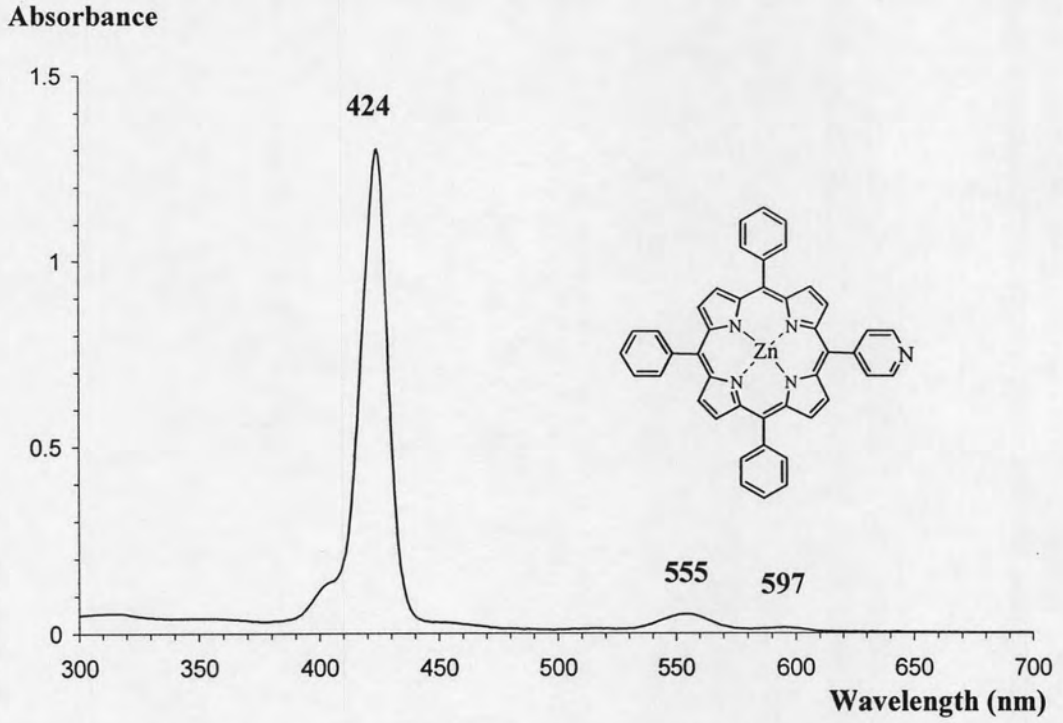

Figure A-35 UV/Visible spectrum of 5-(pyridyl)-10,15,20-triphenylporphyrinato zinc(II) (ZnMPyTPP, **12**)

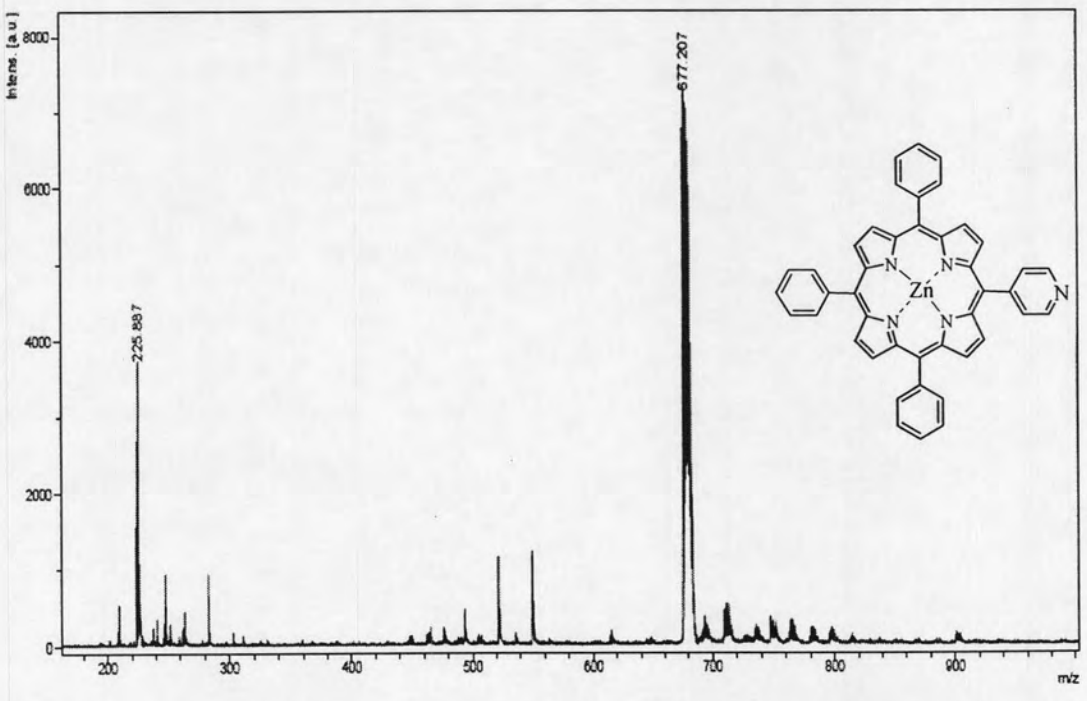

Figure A-36 MALDI-TOF mass spectrum of 5-(pyridyl)-10,15,20-triphenyl porphyrinatozinc(II) (ZnMPyTPP, **12**)

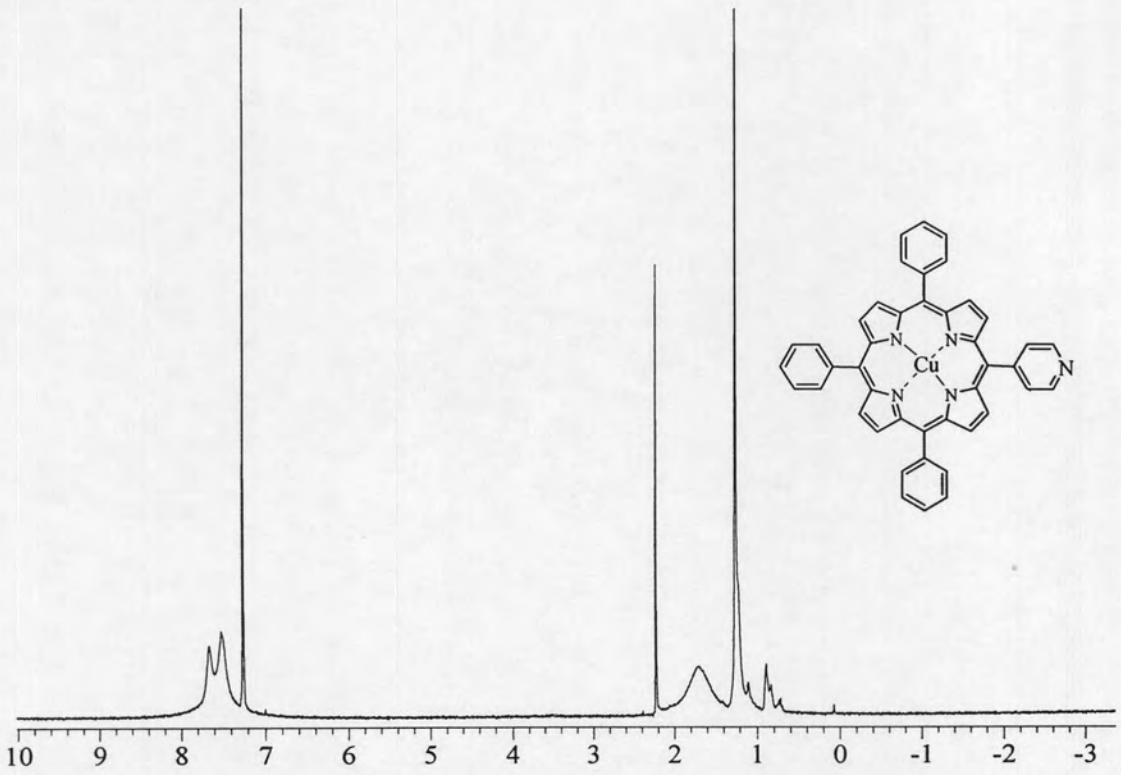

Figure A-37 The ^{1}H NMR spectrum of 5-(pyridyl)-10,15,20-triphenyl porphyrinatocopper(II) (CuMPyTPP, **13**)

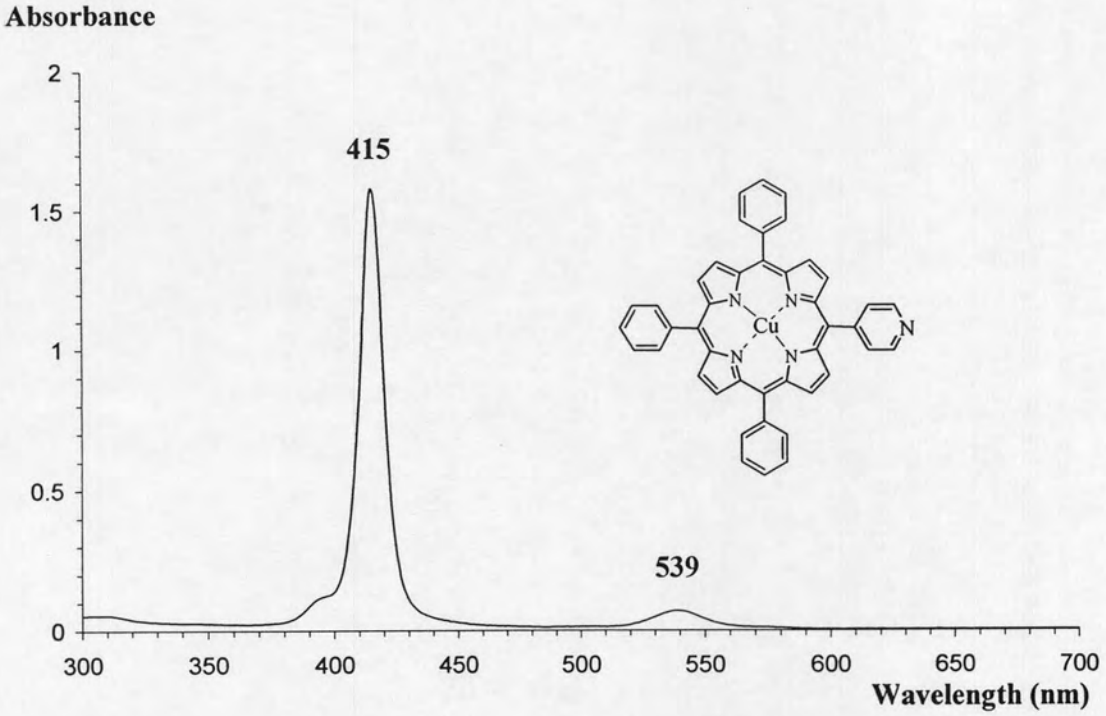

Figure A-38 UV/Visible spectrum of 5-(pyridyl)-10,15,20-triphenylporphyrinato copper(II) (CuMPyTPP, **13**)

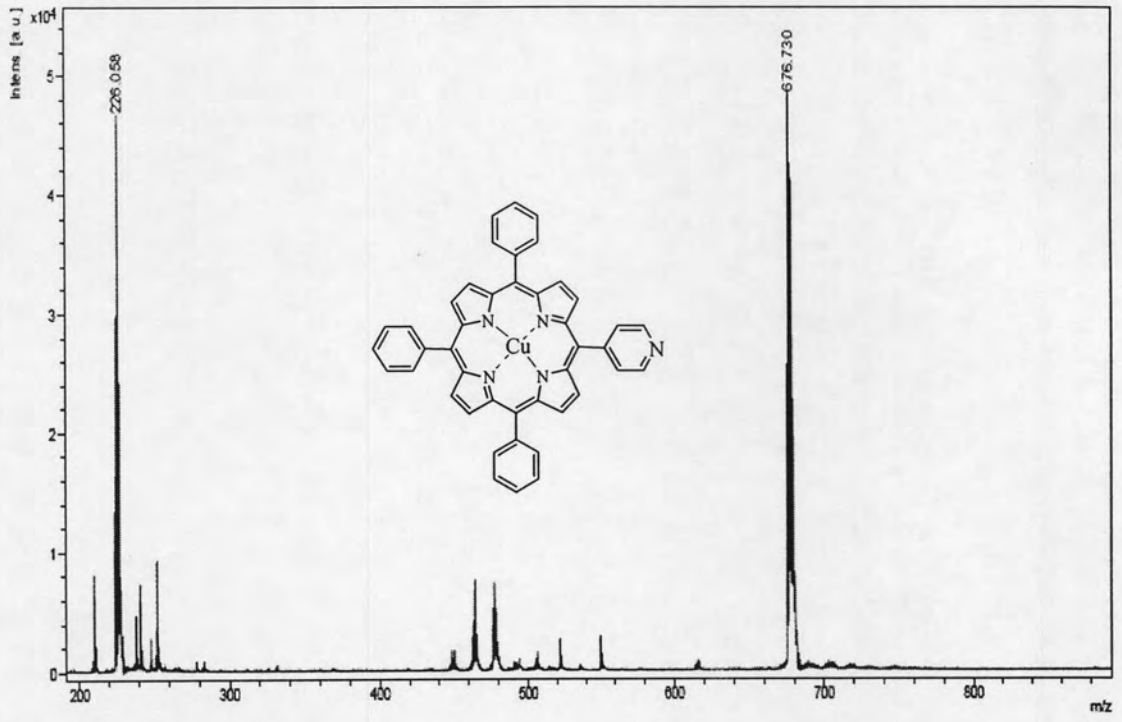

Figure A-39 MALDI-TOF mass spectrum of 5-(pyridyl)-10,15,20-triphenyl porphyrinatocopper(II) (CuMPyTPP, **13**)

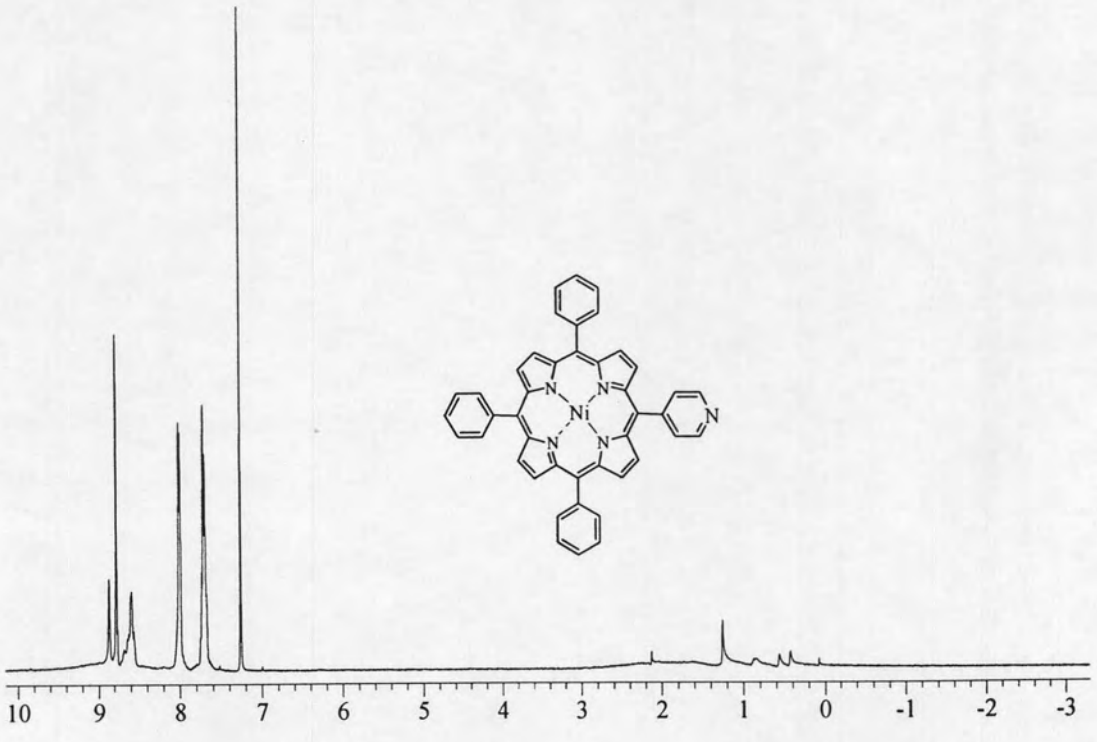

Figure A-40 The ^{1}H NMR spectrum of 5-(pyridyl)-10,15,20-triphenyl porphyrinatonickel(II) (NiMPyTPP, **14**)

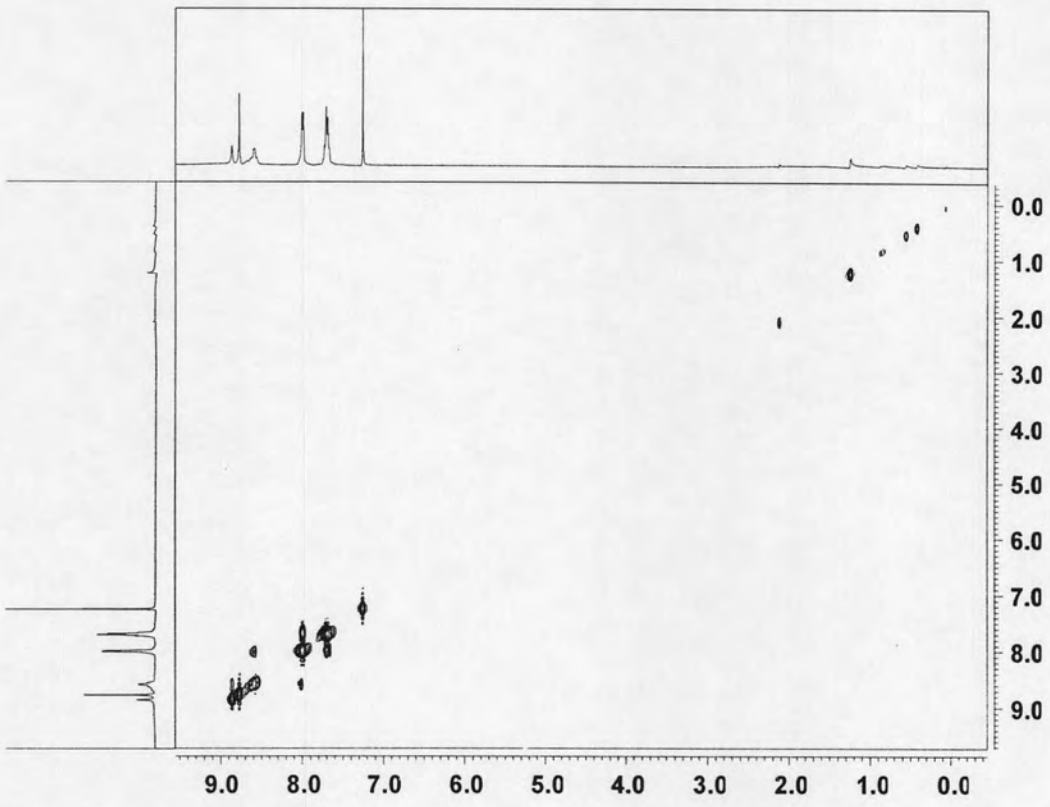

Figure A-41 The ^{1}H-^{1}H COSY spectrum of 5-(pyridyl)-10,15,20-triphenyl porphyrinatonickel(II) (NiMPyTPP, **14**)

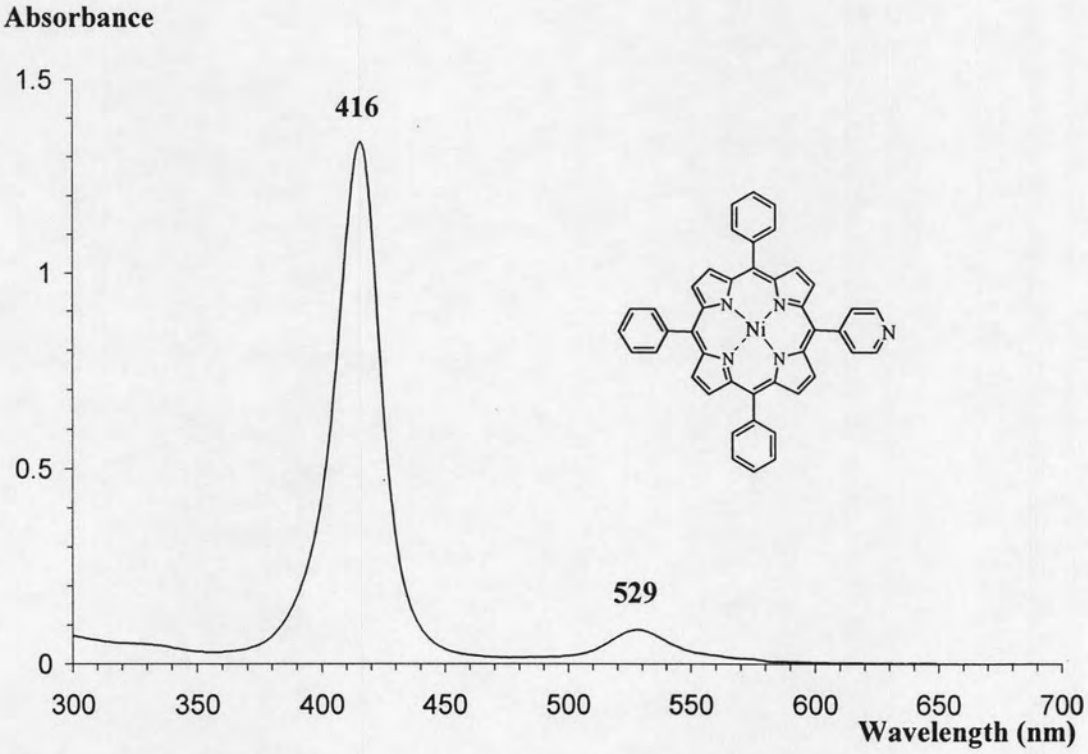

Figure A-42 UV/Visible spectrum of 5-(pyridyl)-10,15,20-triphenylporphyrinato nickel(II) (NiMPyTPP, **14**)

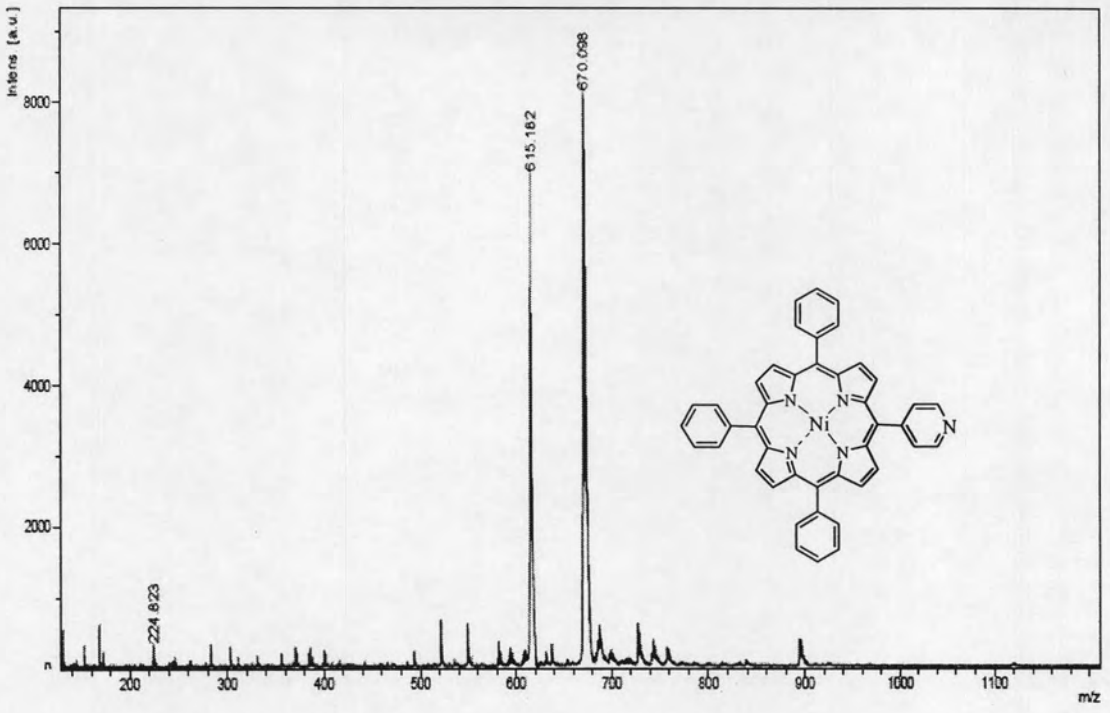

Figure A-43 MALDI-TOF mass spectrum of 5-(pyridyl)-10,15,20-triphenyl porphyrinatonickel(II) (NiMPyTPP, **14**)

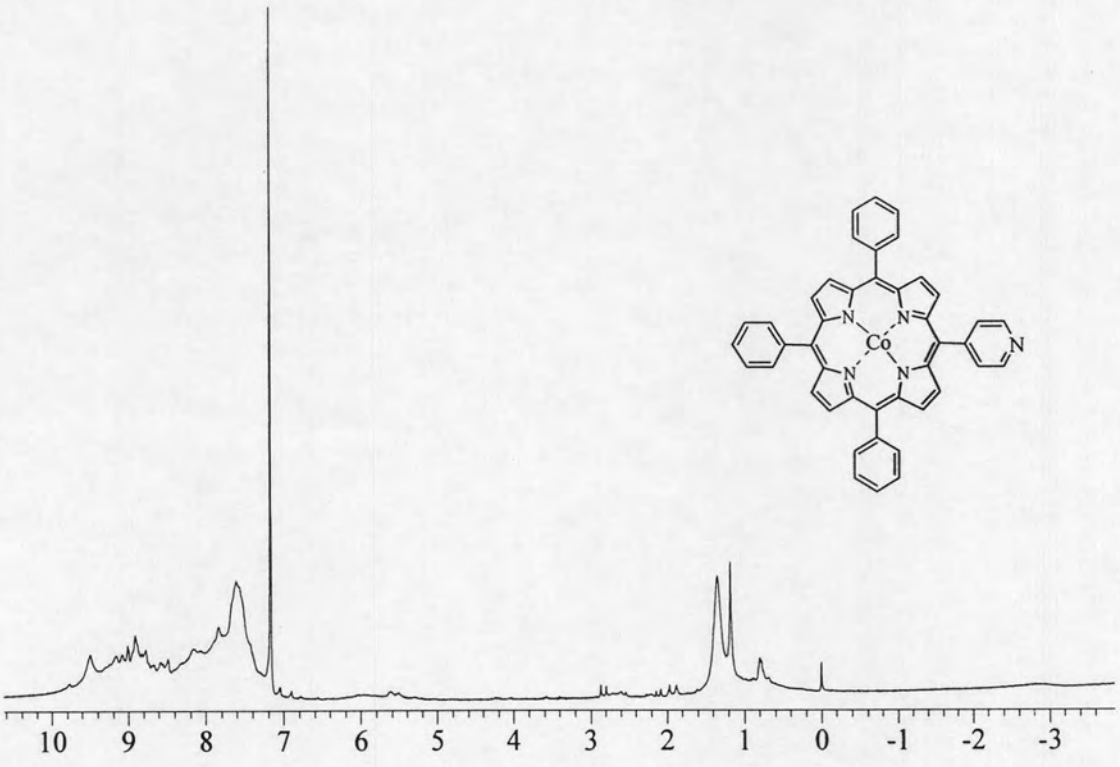

Figure A-44 The ^{1}H NMR spectrum of 5-(pyridyl)-10,15,20-triphenyl porphyrinatocobalt(II) (CoMPyTPP, **15**)

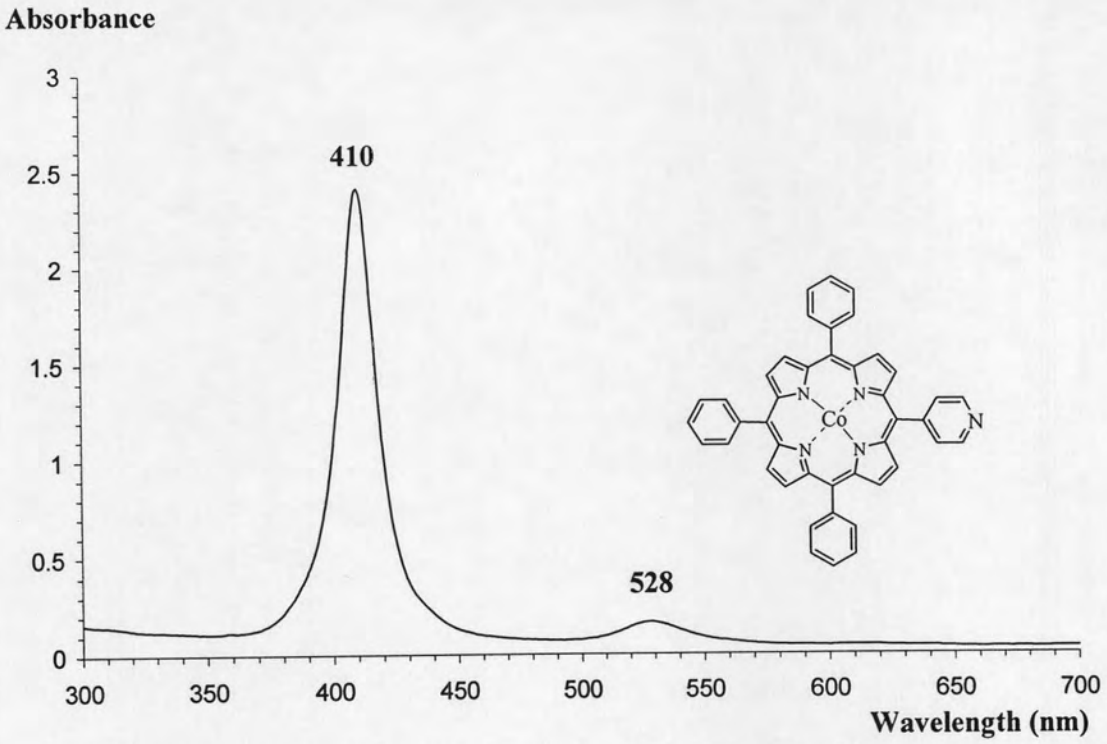

Figure A-45 UV/Visible spectrum of 5-pyridyl-10,15,20-triphenylporphyrinato cobalt(II) (CoMPyTPP, **15**)

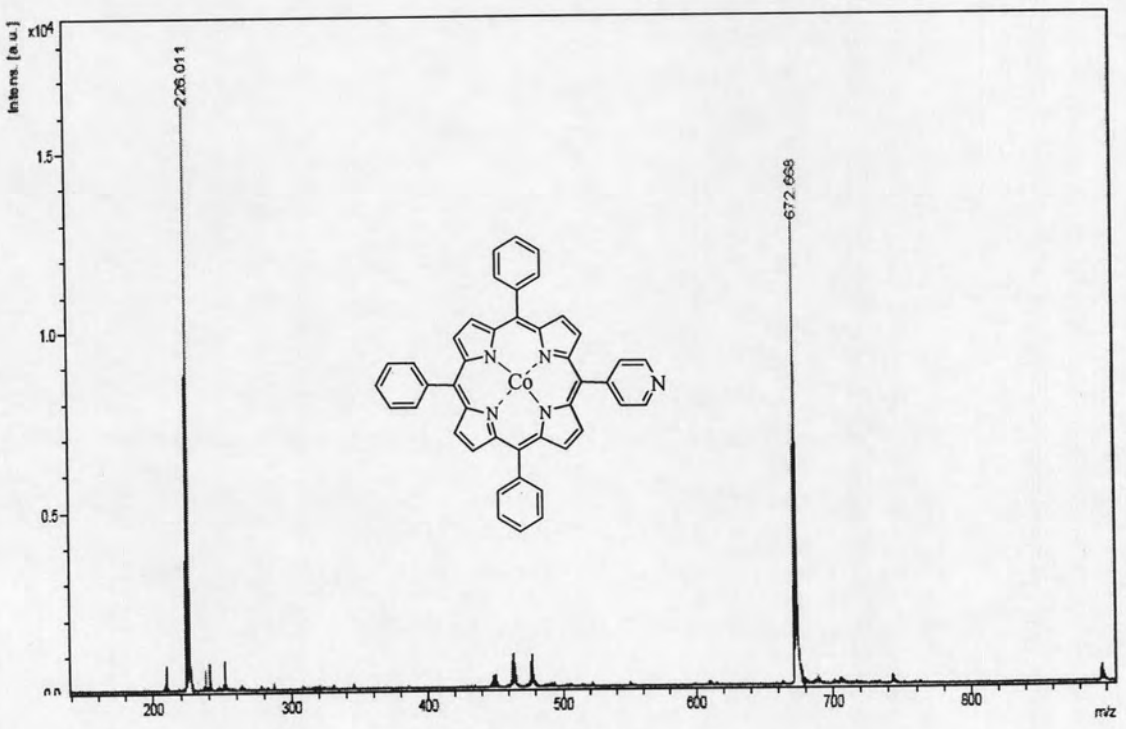

Figure A-46 MALDI-TOF mass spectrum of 5-(pyridyl)-10,15,20-triphenyl porphyrinatocobalt(II) (CoMPyTPP, **15**)

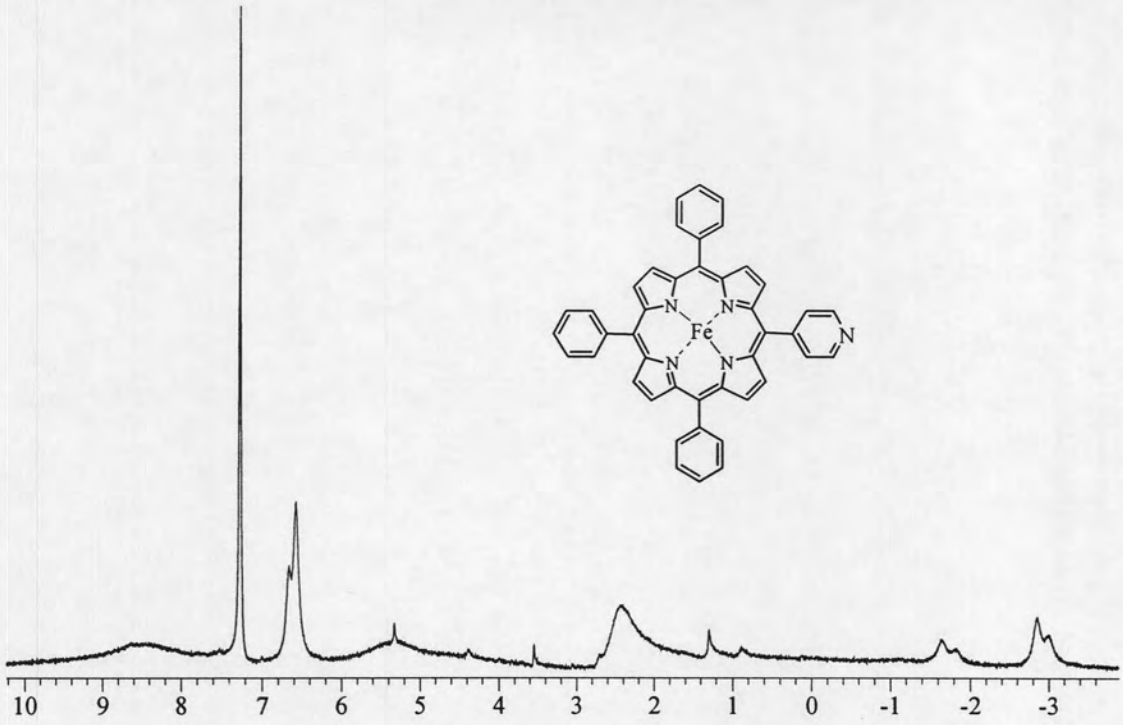

Figure A-47 The ^{1}H NMR spectrum of 5-pyridyl-10,15,20-triphenyl porphyrinatoiron(III) ((Cl)FeMPyTPP, **16**)

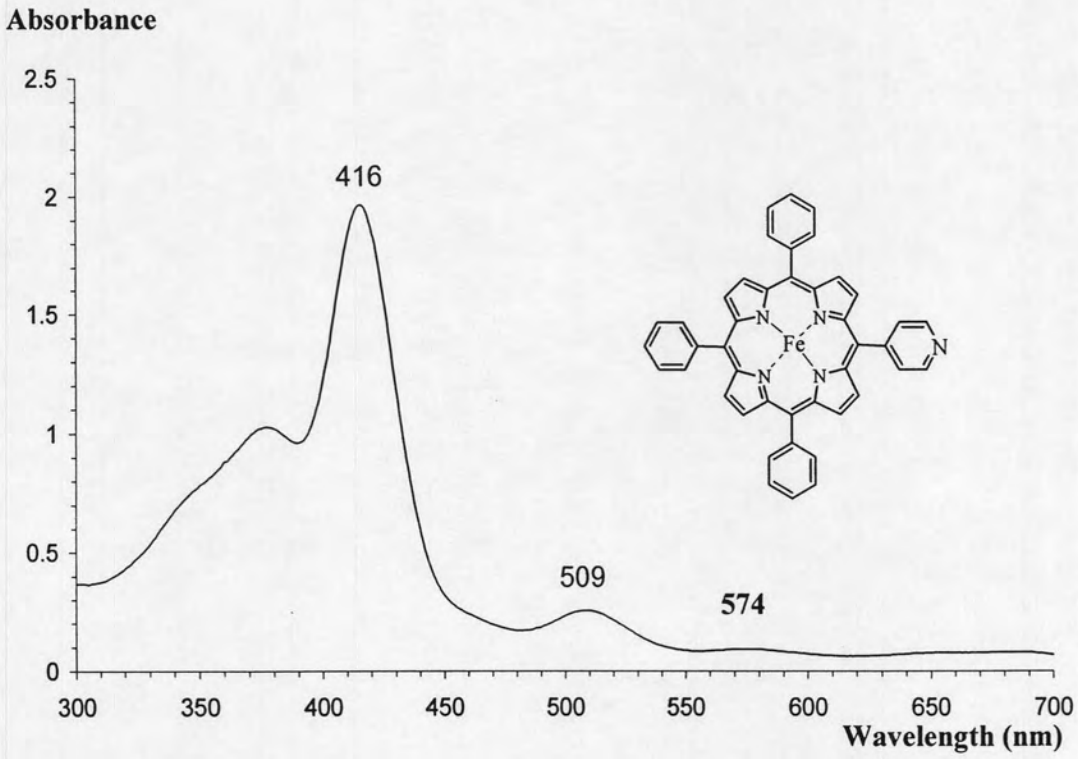

Figure A-48 UV/Visible spectrum of 5-pyridyl-10,15,20-triphenylporphyrinato iron(III) ((Cl)FeMPyTPP, **16**)

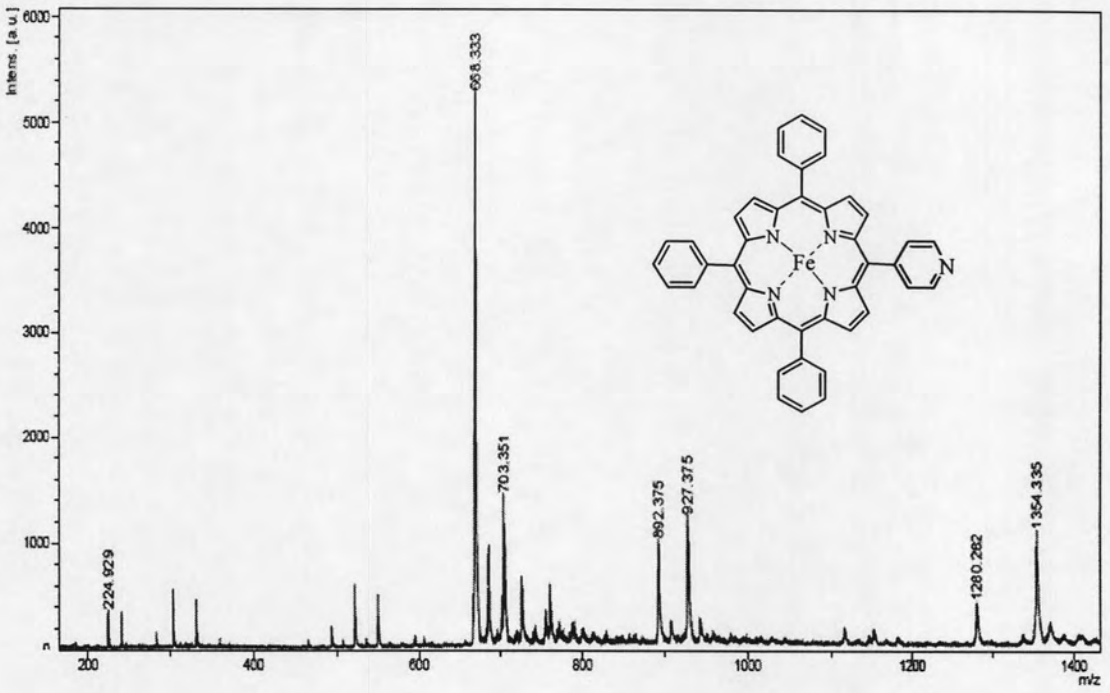

Figure A-49 MALDI-TOF mass spectrum of 5-(pyridyl)-10,15,20-triphenyl porphyrinato(III) ((Cl)FeMPyTPP, **16**)

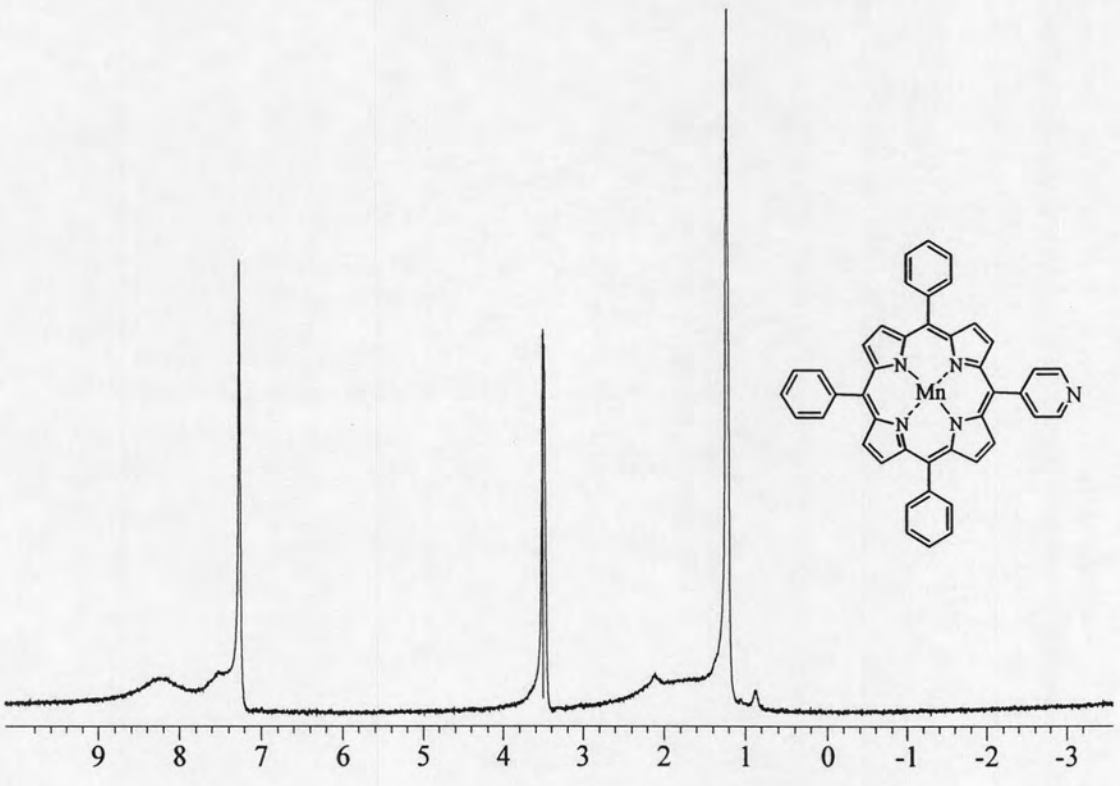

Figure A-50 The ^{1}H NMR spectrum of 5-(pyridyl)-10,15,20-triphenylporphyrinato manganese(III) (MnMPyTPP, **17**)

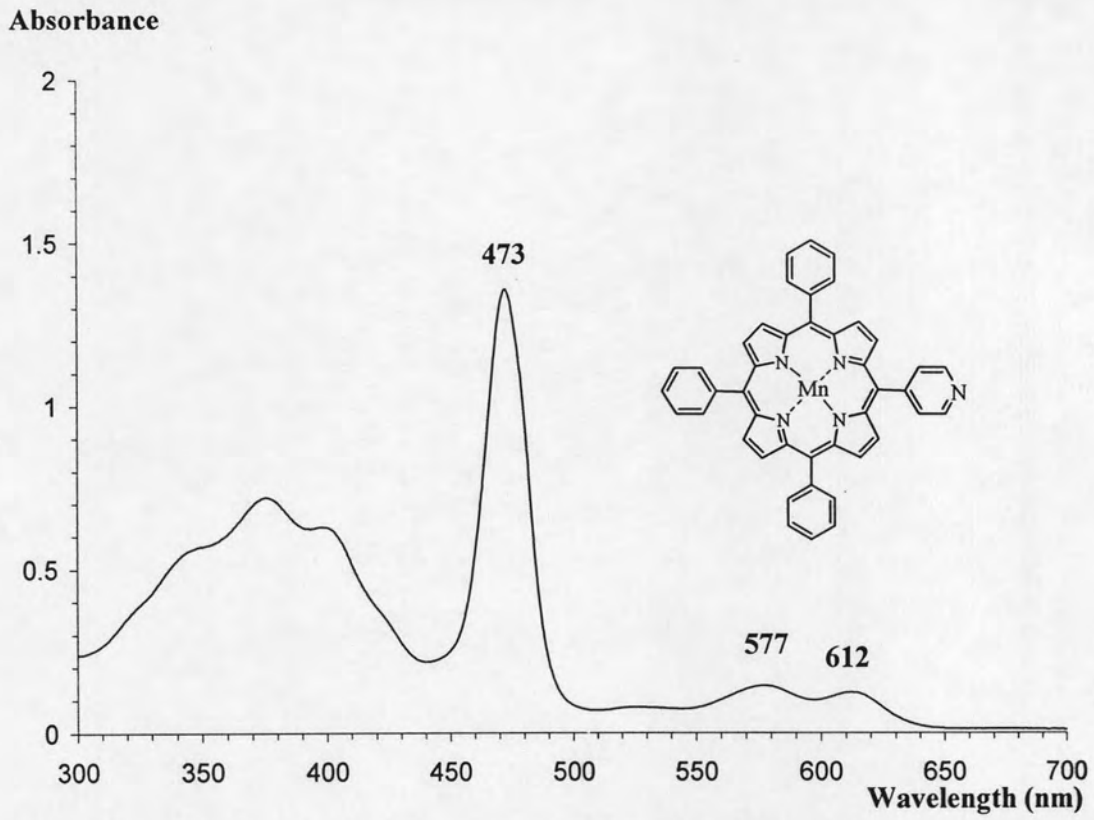

Figure A-51 UV/Visible spectrum of 5-(pyridyl)-10,15,20-triphenyl porphyrinatomanganese(III) (MnMPyTPP, **17**)

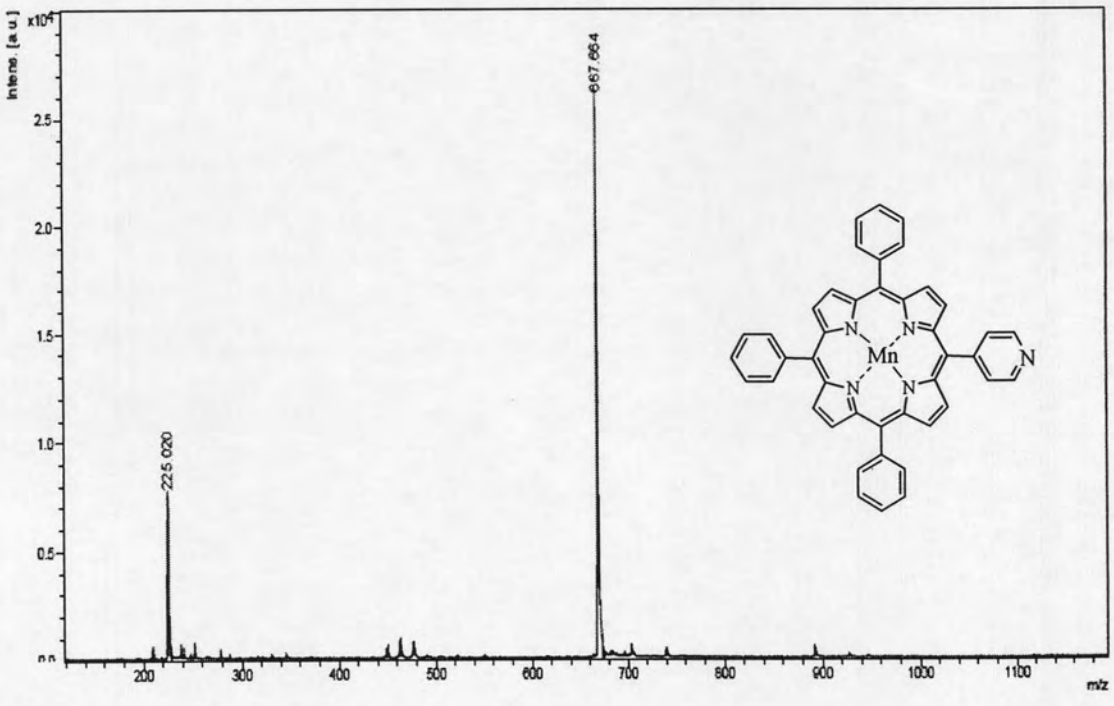

Figure A-52 MALDI-TOF mass spectrum of 5-(pyridyl)-10,15,20-triphenyl porphyrinatomanganese(III) (MnMPyTPP, **17**)

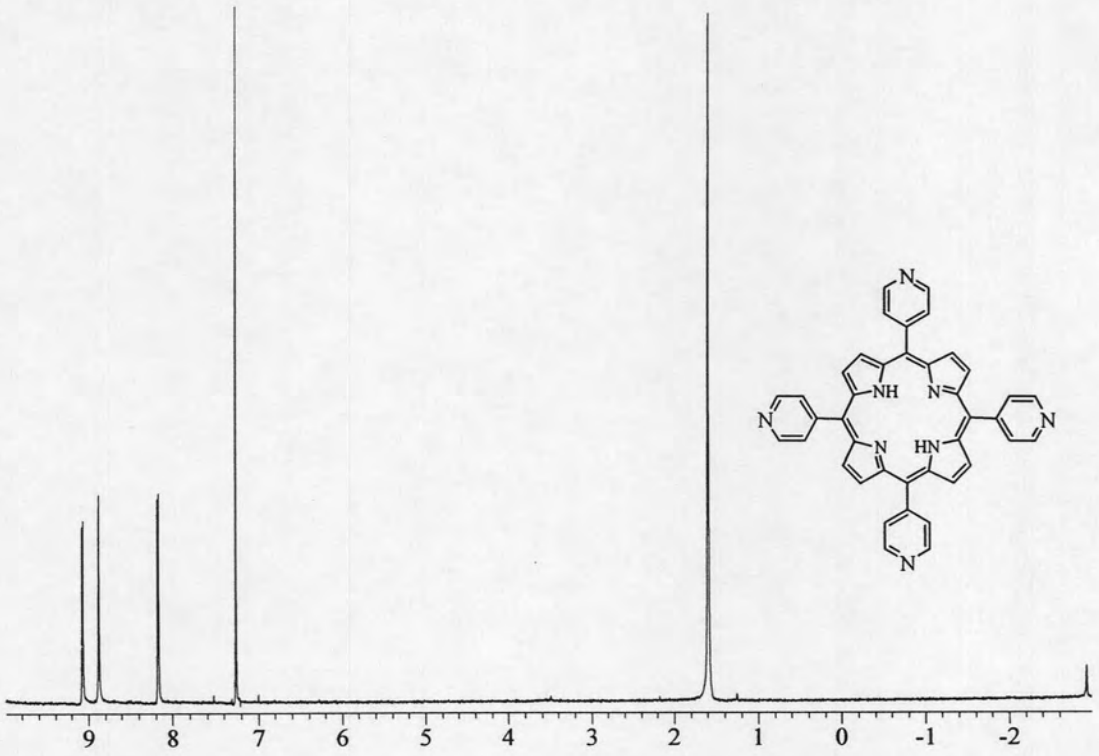

Figure A-53 The ^{1}H NMR spectrum of 5,10,15,20-tetrapyridylporphyrin (TPyP, **18**)

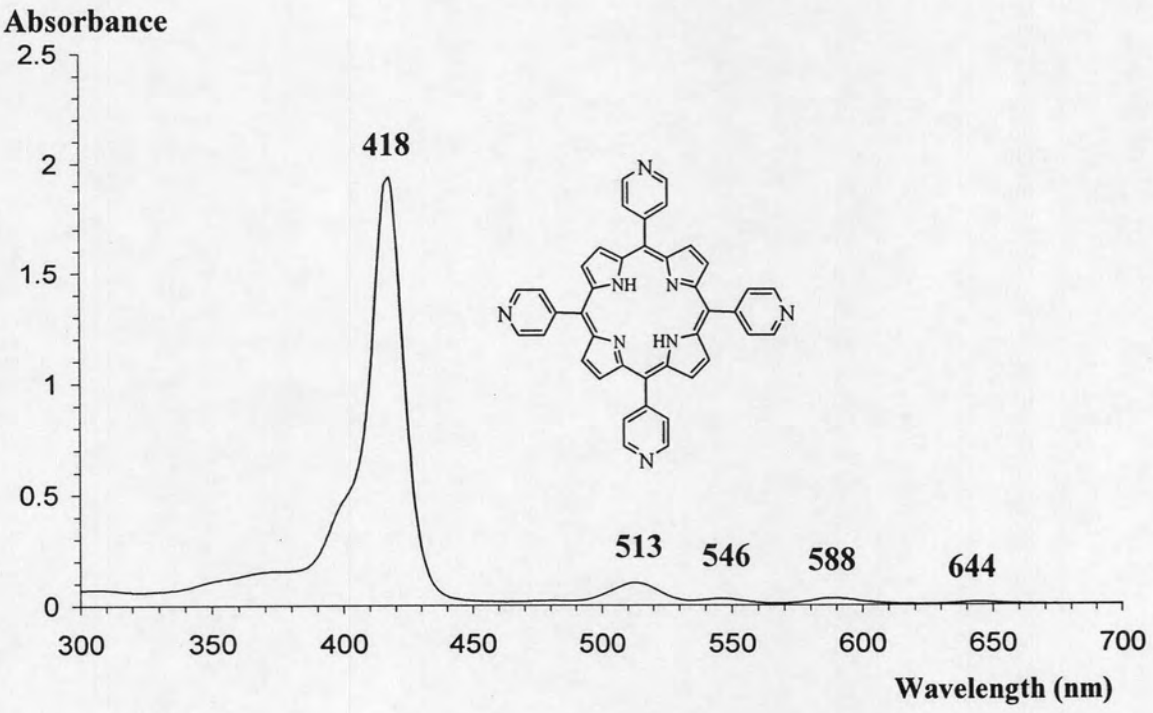

Figure A-54 UV/Visible spectrum of 5,10,15,20-tetrapyridylporphyrin (TPyP, **18**)

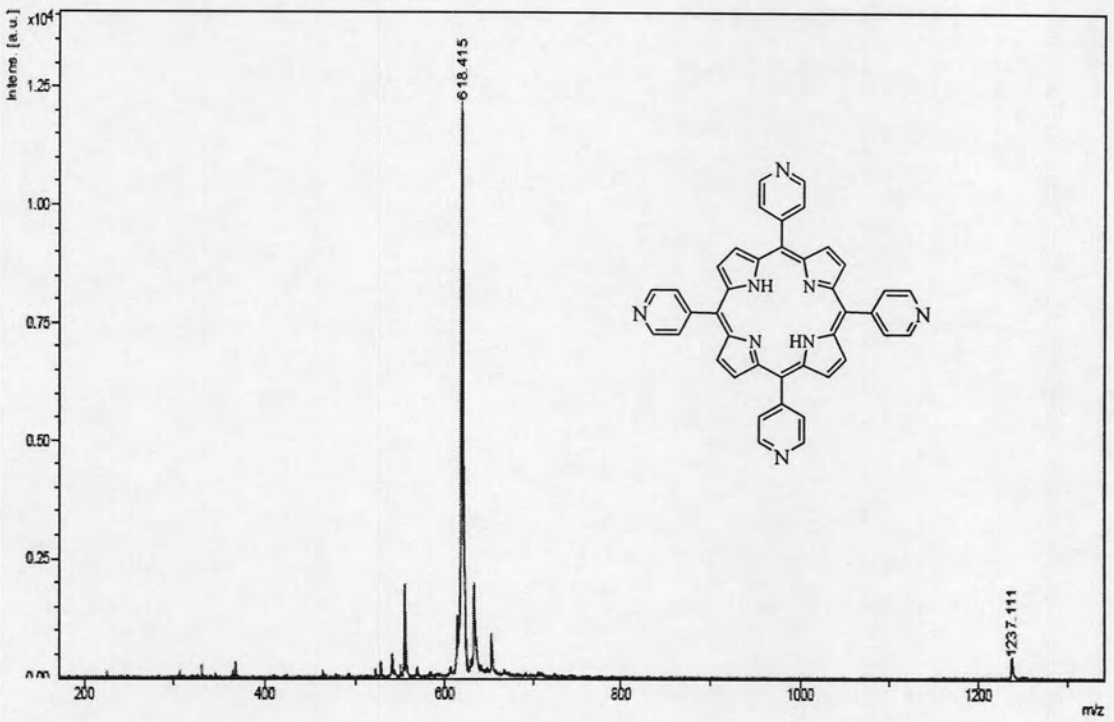

Figure A-55 MALDI-TOF mass spectrum of 5,10,15,20-tetrapyridylporphyrin (TPyP, **18**)

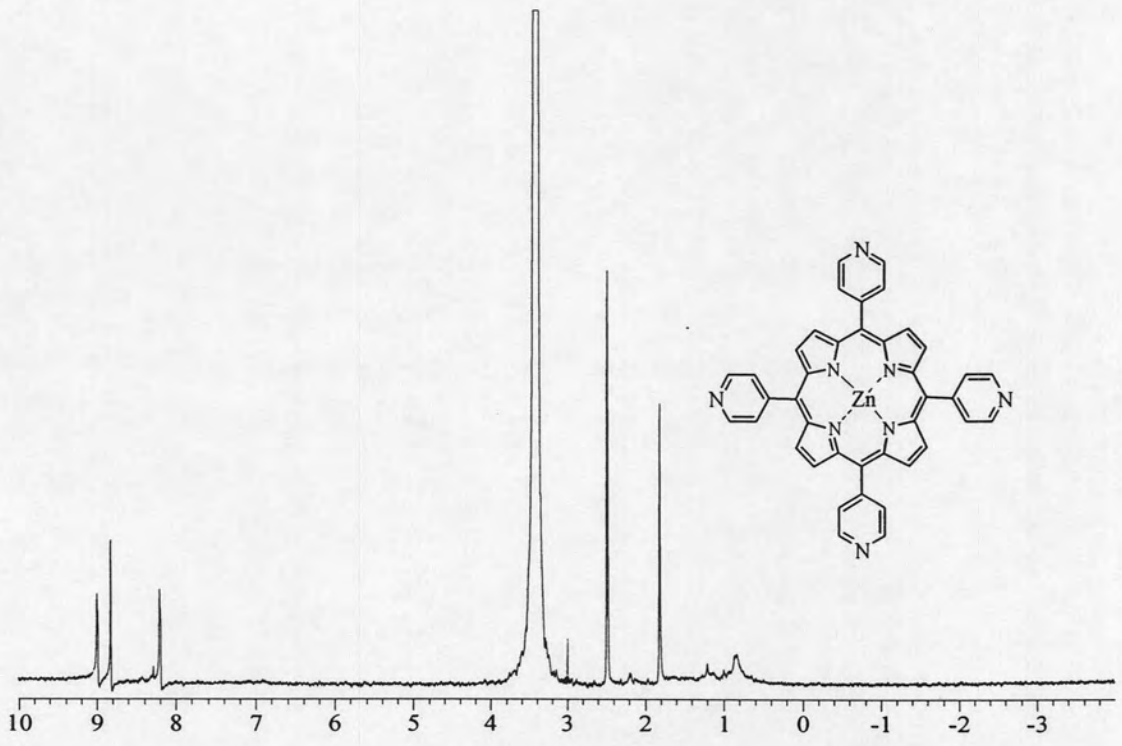

Figure A-56 The ^{1}H NMR spectrum of 5,10,15,20-tetrapyridylporphyrinatozinc(II) (ZnTPyP, **19**)

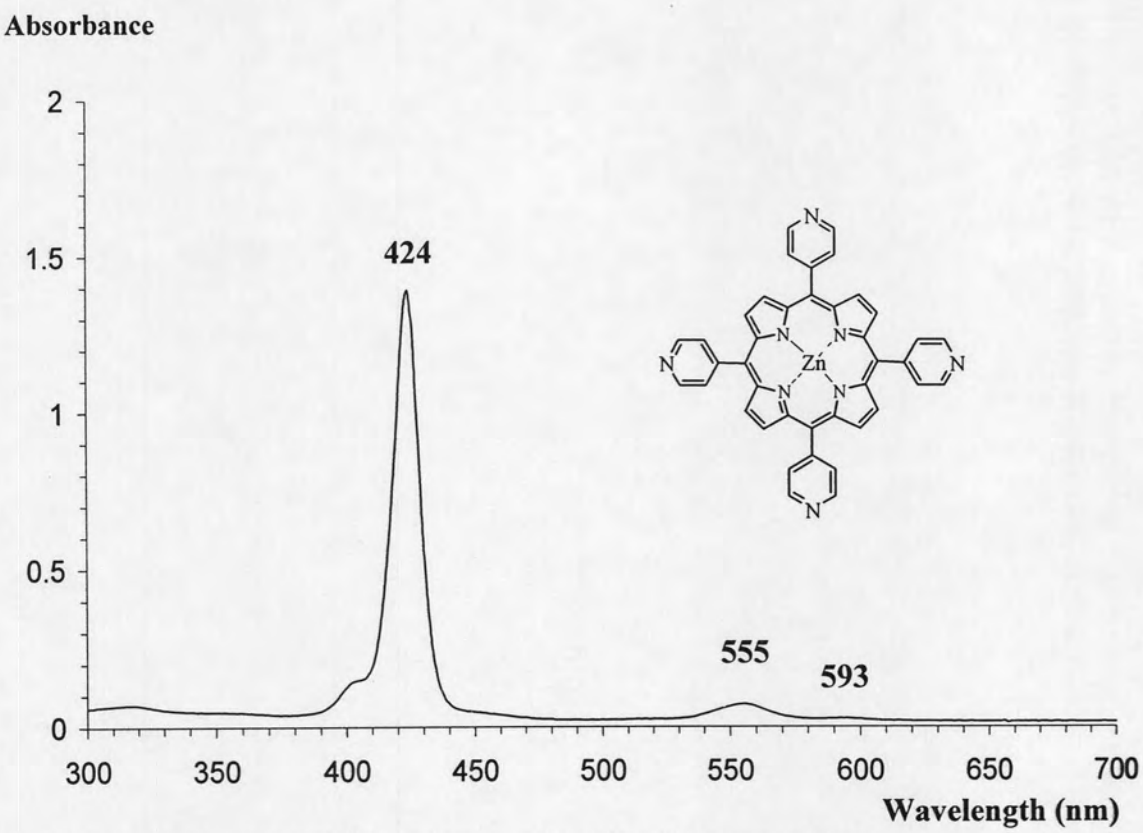

Figure A-57 UV/Visible spectrum of 5,10,15,20-tetrapyridylporphyrinatozinc(II) (ZnTPyP, **19**)

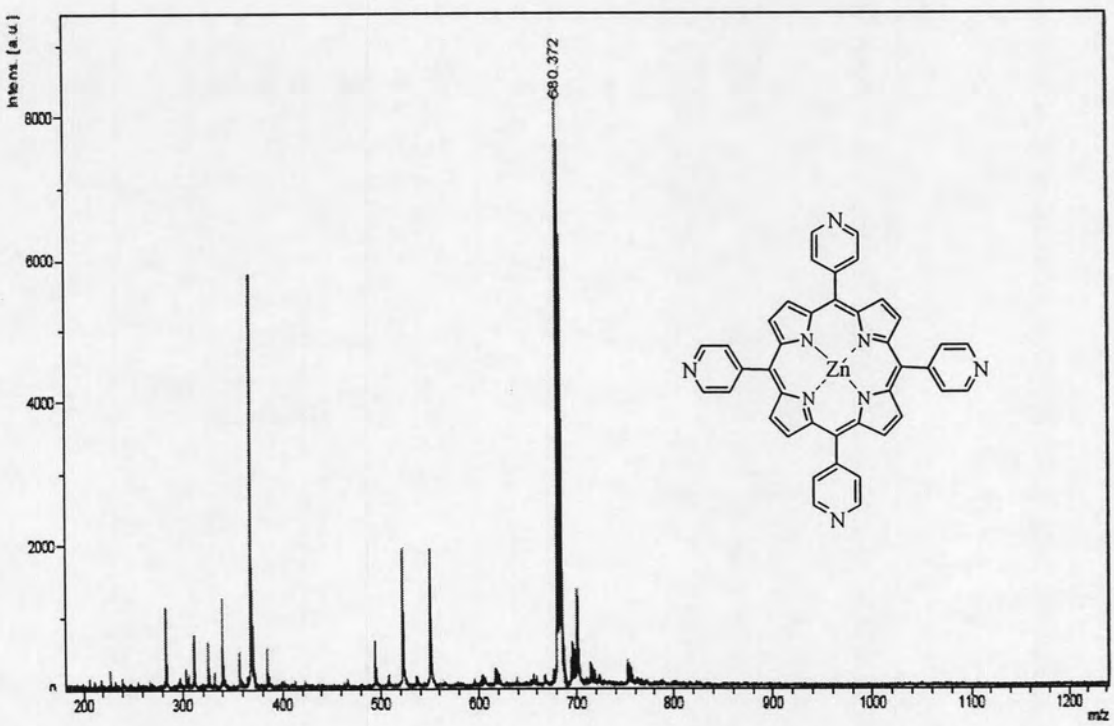

Figure A-58 MALDI-TOF mass spectrum of 5,10,15,20-tetrapyridyl porphyrinatozinc(II) (ZnTPyP, **19**)

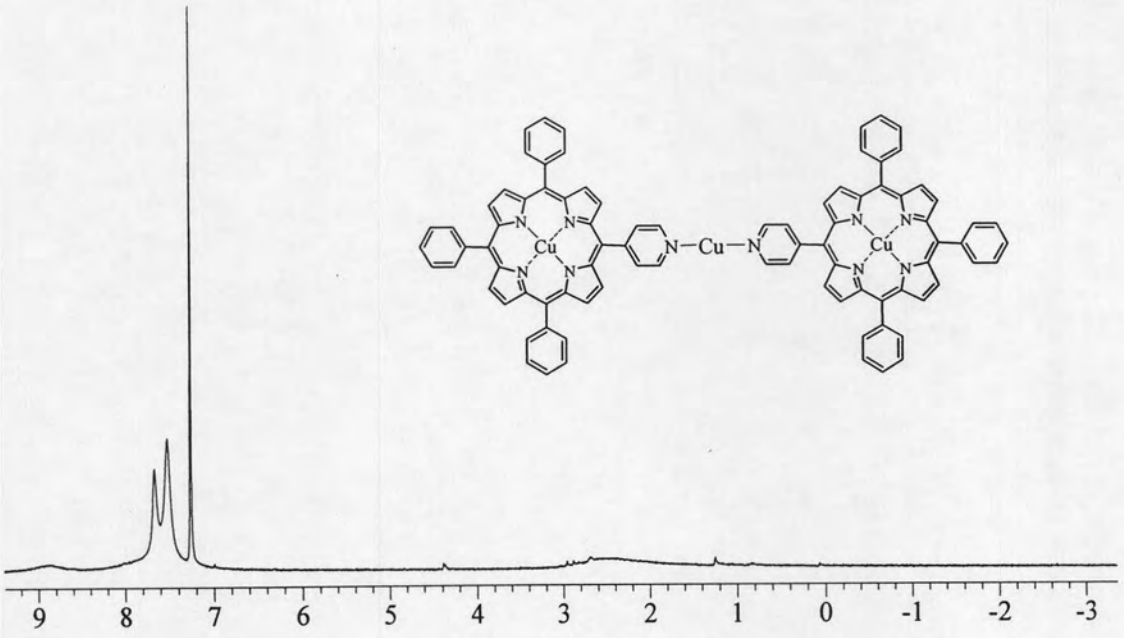

Figure A-59 The ^{1}H NMR spectrum of Cu(II)(CuMPyTPP)$_2$ (**20**)

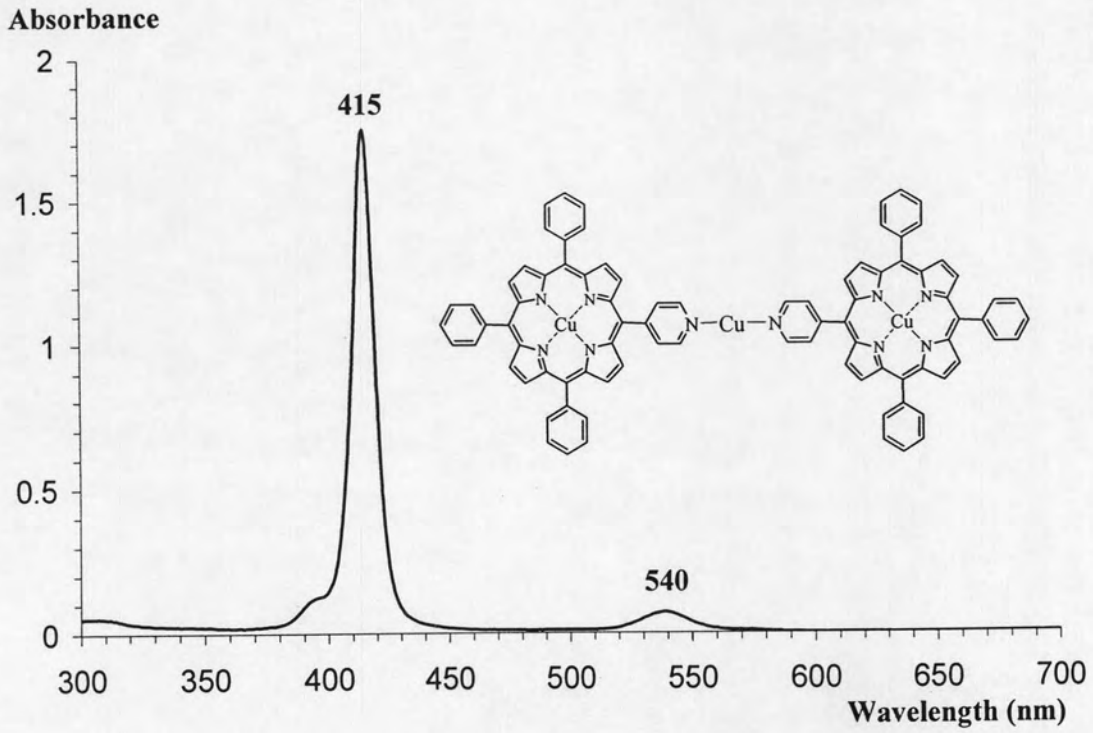

Figure A-60 UV/Visible spectrum of Cu(II)(CuMPyTPP)$_2$ (**20**)

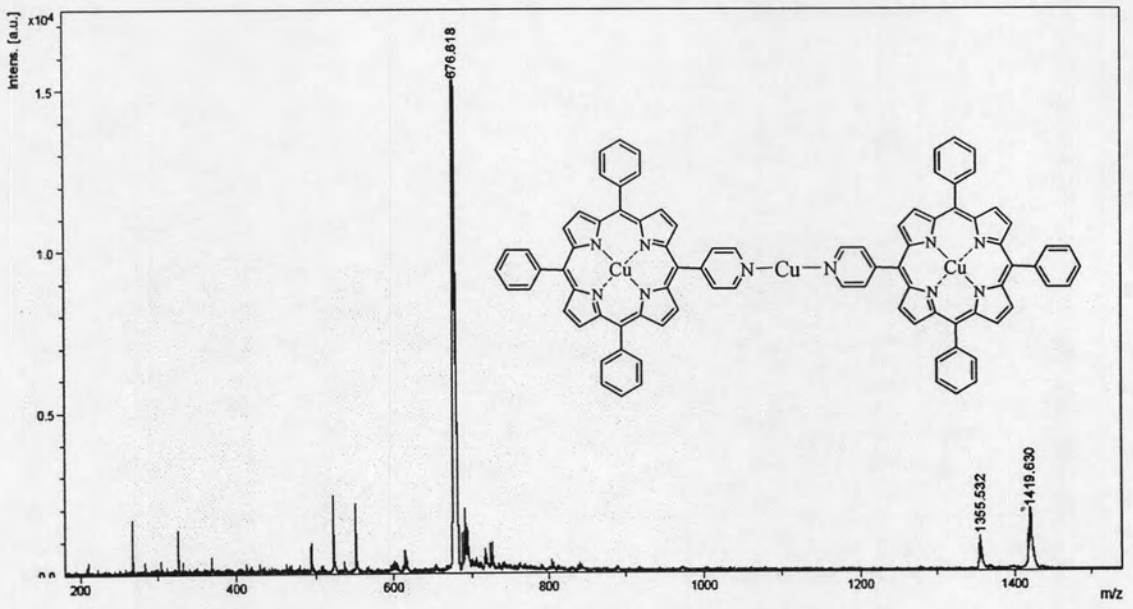

Figure A-61 MALDI-TOF mass spectrum of Cu(II)(CuMPyTPP)$_2$ (**20**)

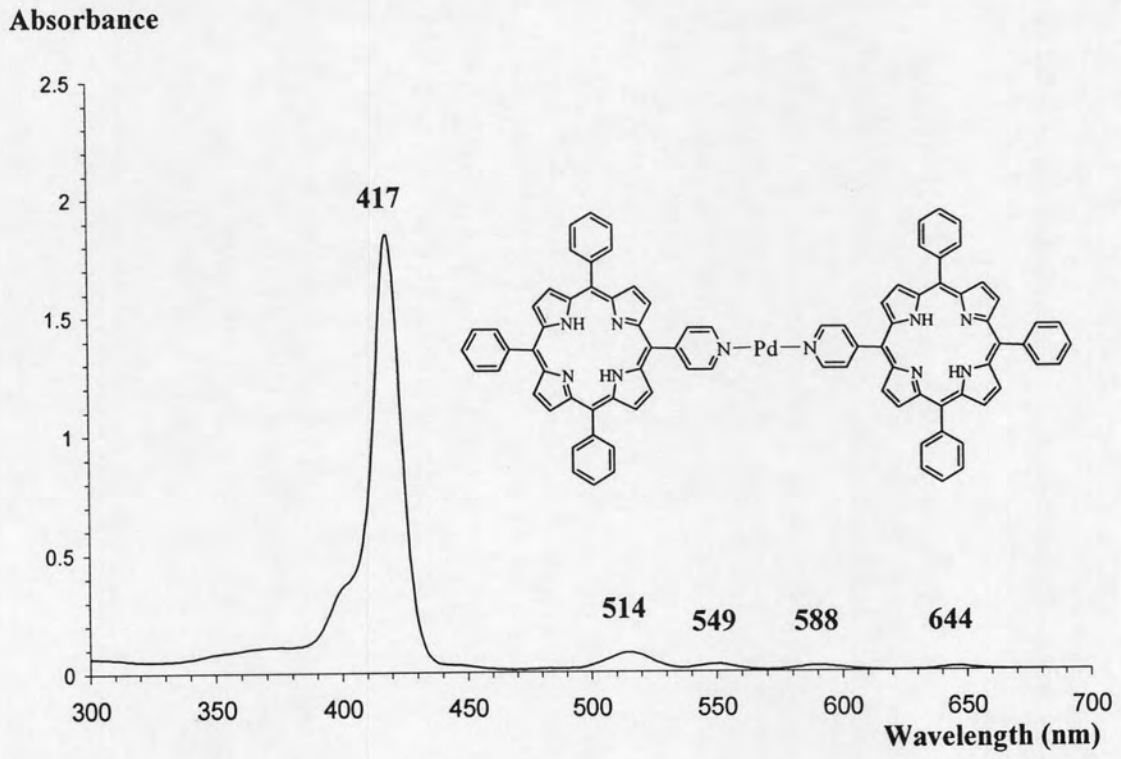

Figure A-62 UV/Visible spectrum of Pd(II)(MPyTPP)$_2$ (**21**)

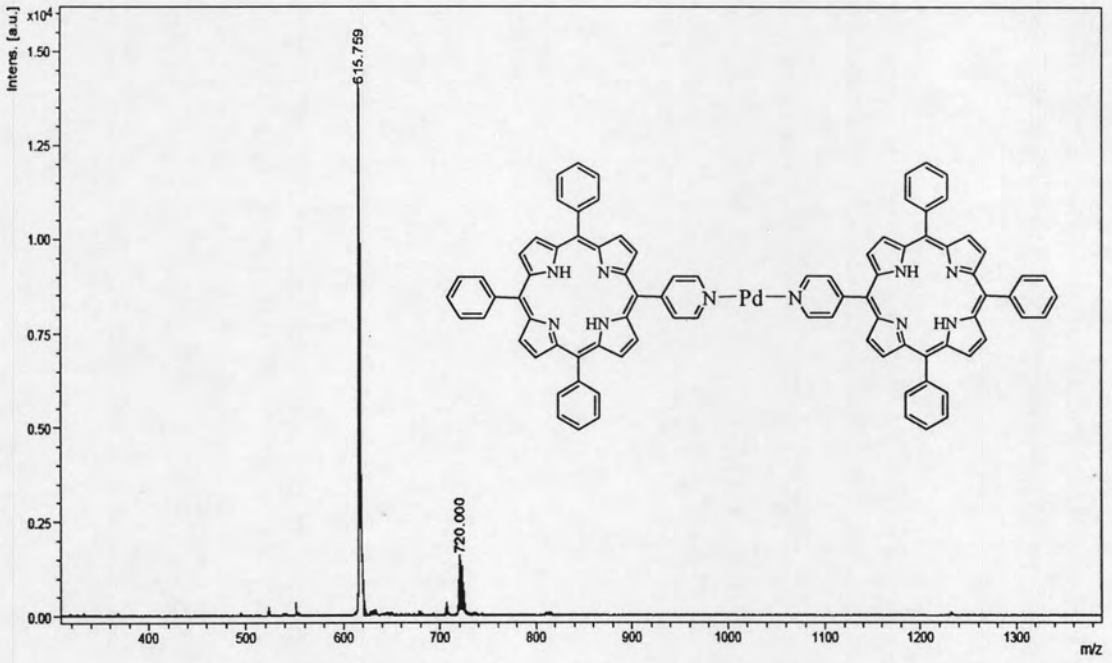

Figure A-63 MALDI-TOF mass spectrum of Pd(II)(MPyTPP)$_2$ (**21**)

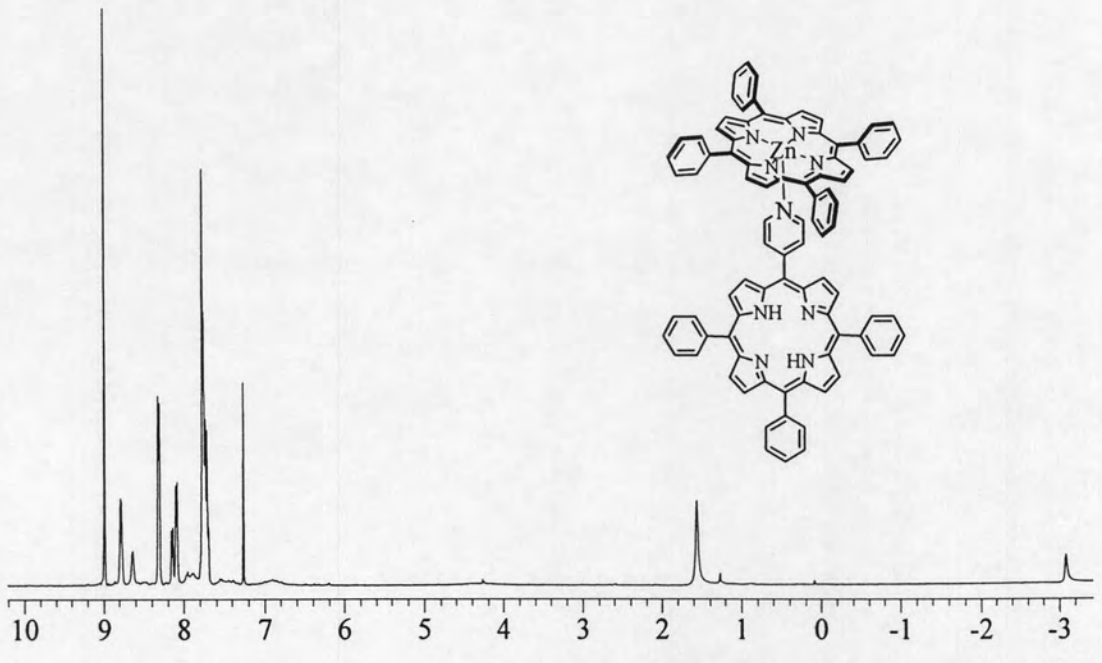

Figure A-64 The ^{1}H NMR spectrum of Zn(TPP)(MPyTPP), (**22**)

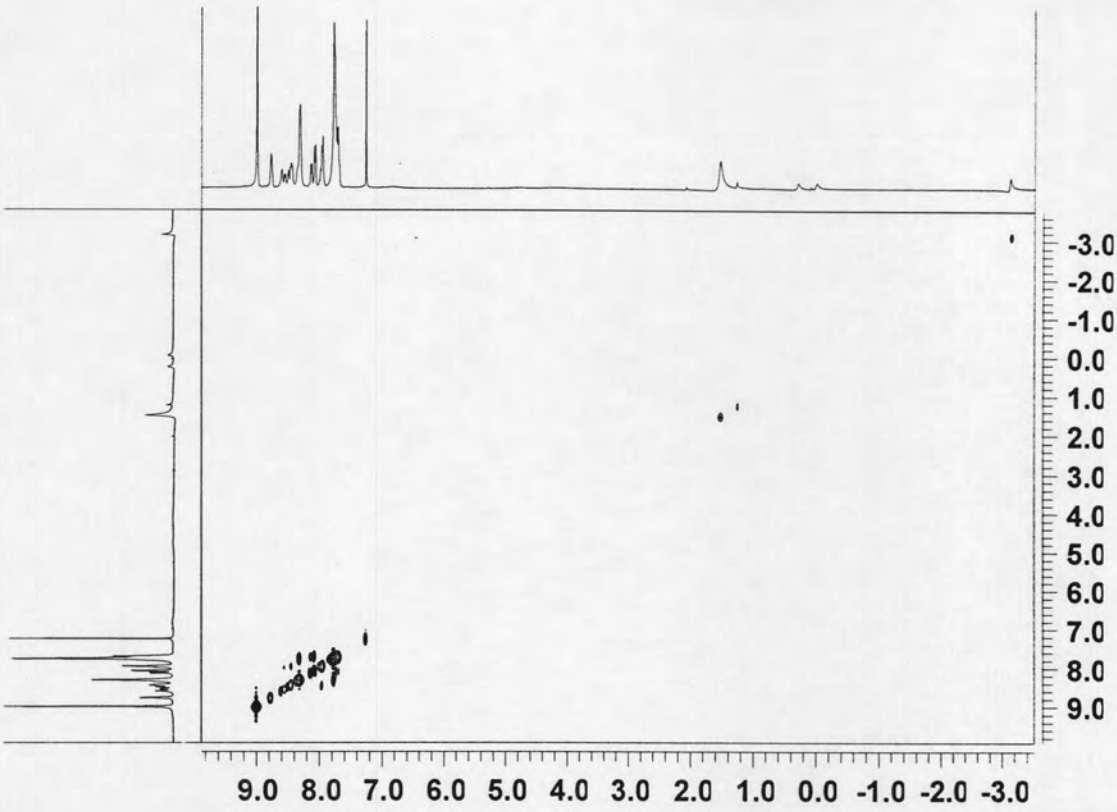

Figure A-65 The ^{1}H-^{1}H COSY spectrum of Zn(TPP)(MPyTPP), (**22**)

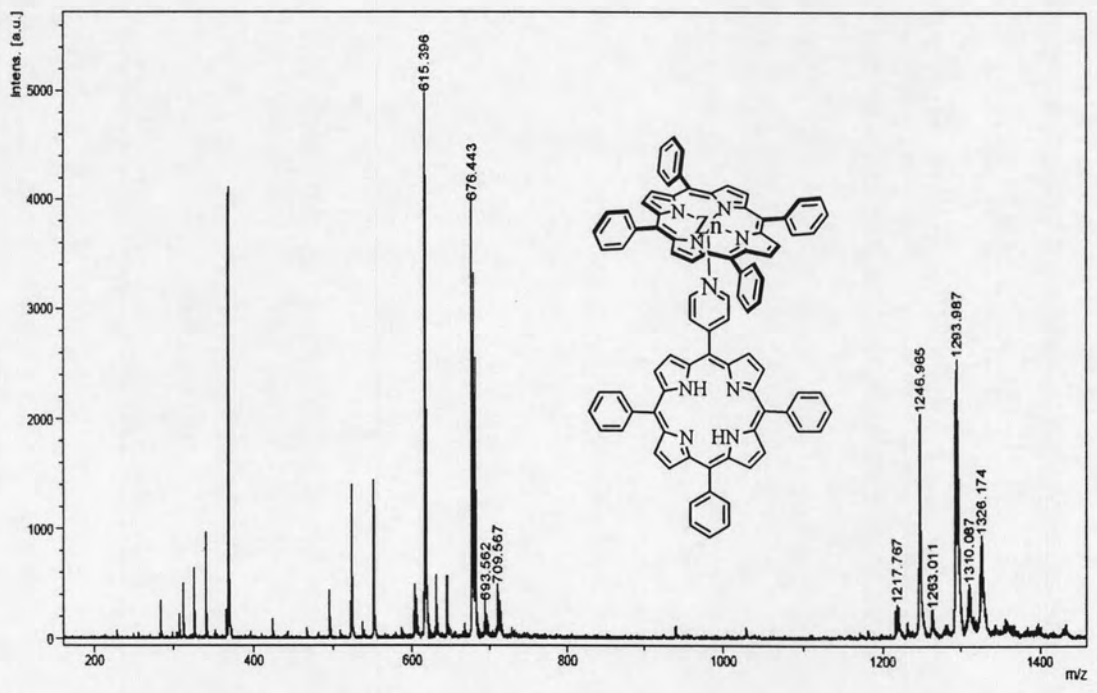

Figure A-66 MALDI-TOF mass spectrum of Zn(TPP)(MPyTPP), (**22**)

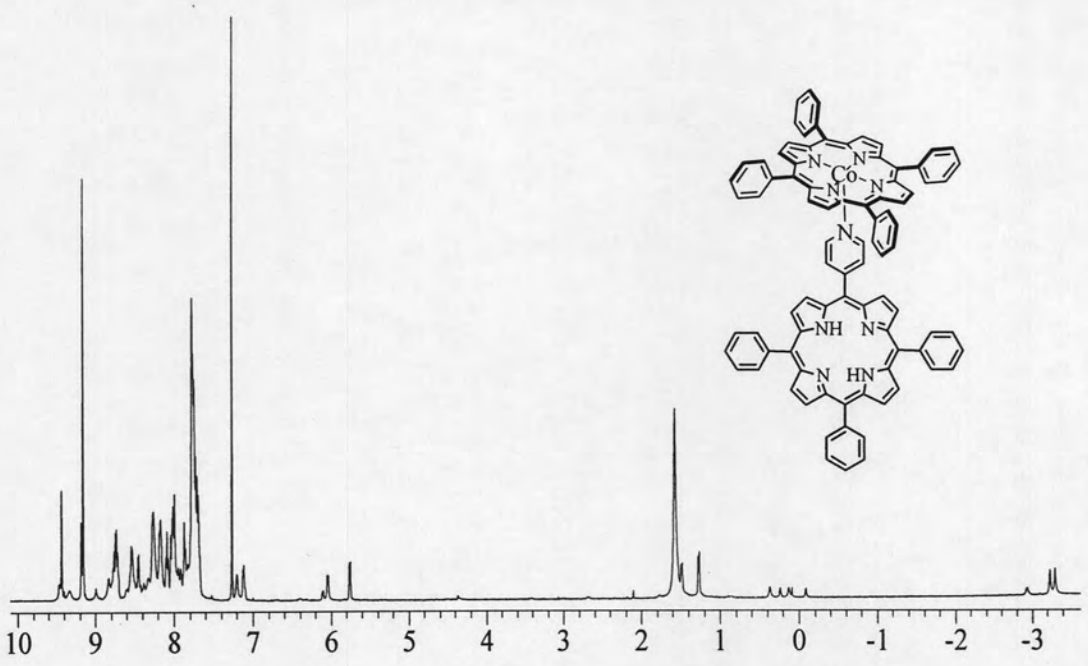

Figure A-67 The ^{1}H NMR spectrum of Co(TPP)(MPyTPP), (**23**)

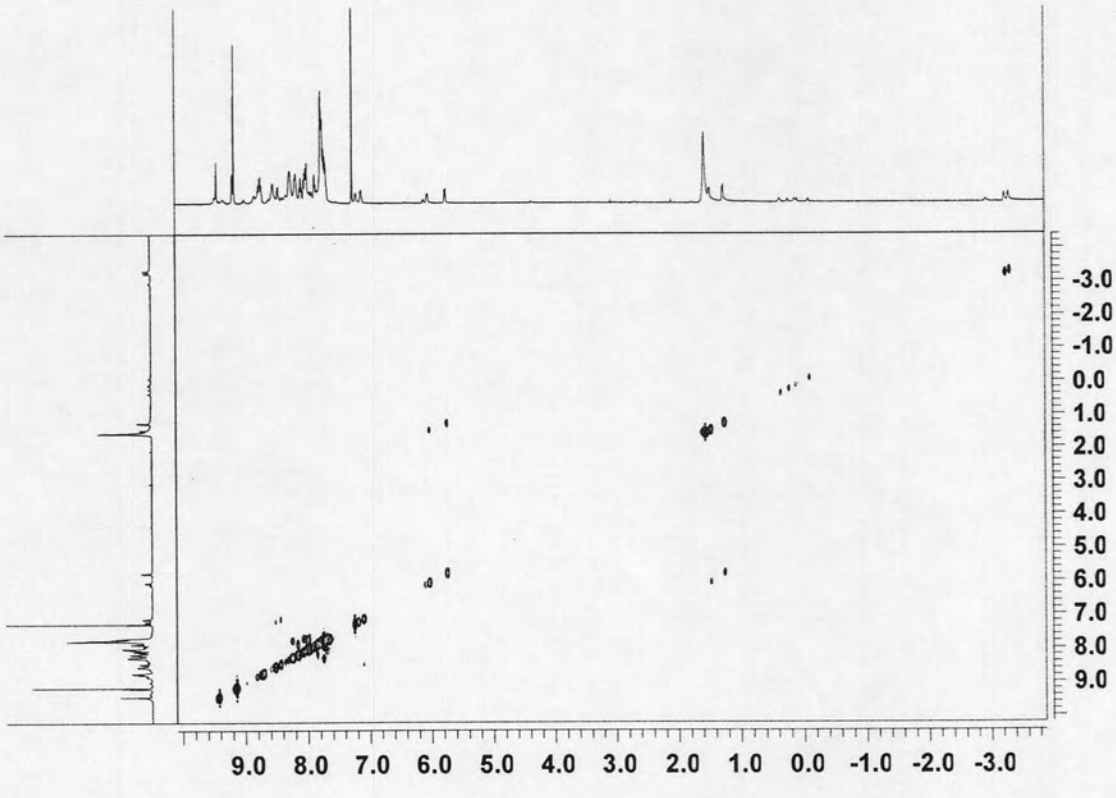

Figure A-68 The ^{1}H-^{1}H COSY spectrum of Co(TPP)(MPyTPP), (**23**)

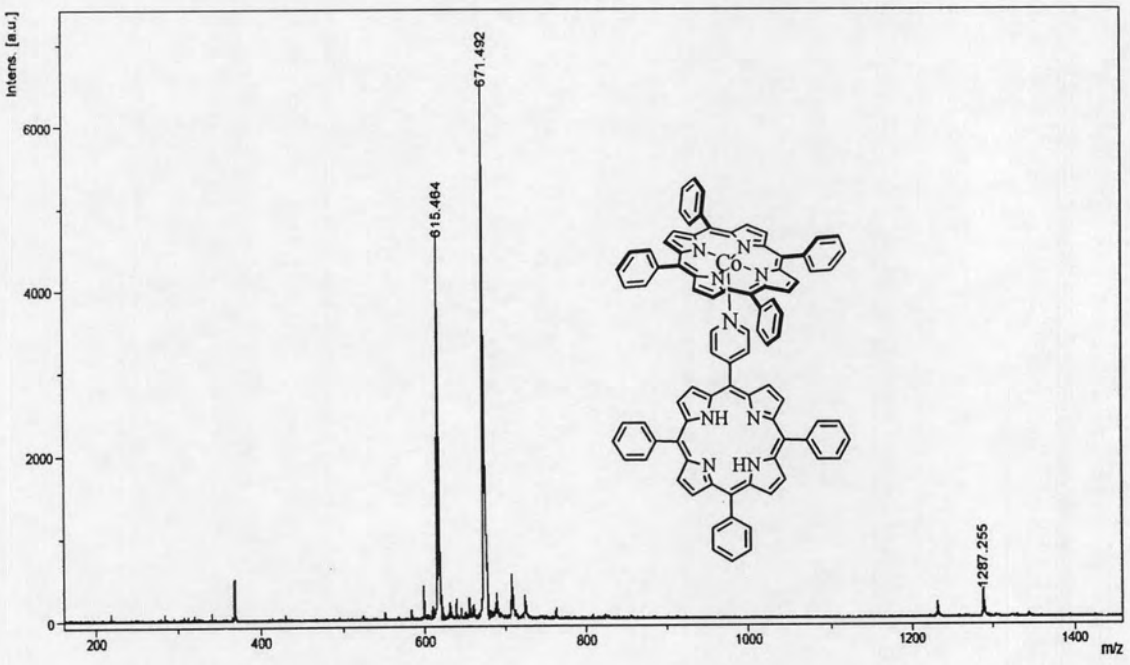

Figure A-69 MALDI-TOF mass spectrum of Co(TPP)(MPyTPP), (**23**)

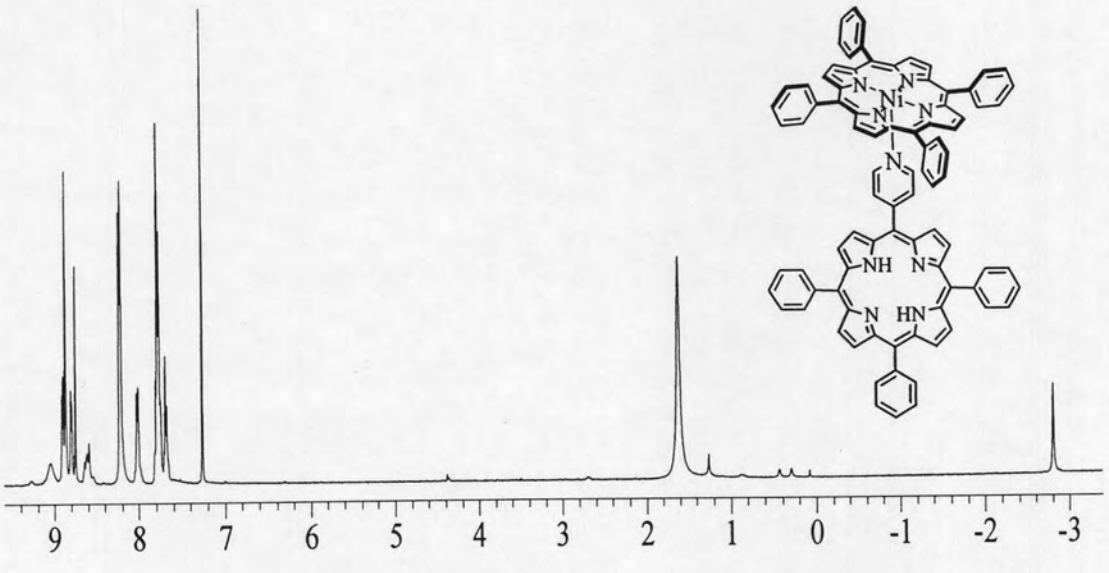

Figure A-70 The ^{1}H NMR spectrum of Ni(TPP)(MPyTPP), (**24**)

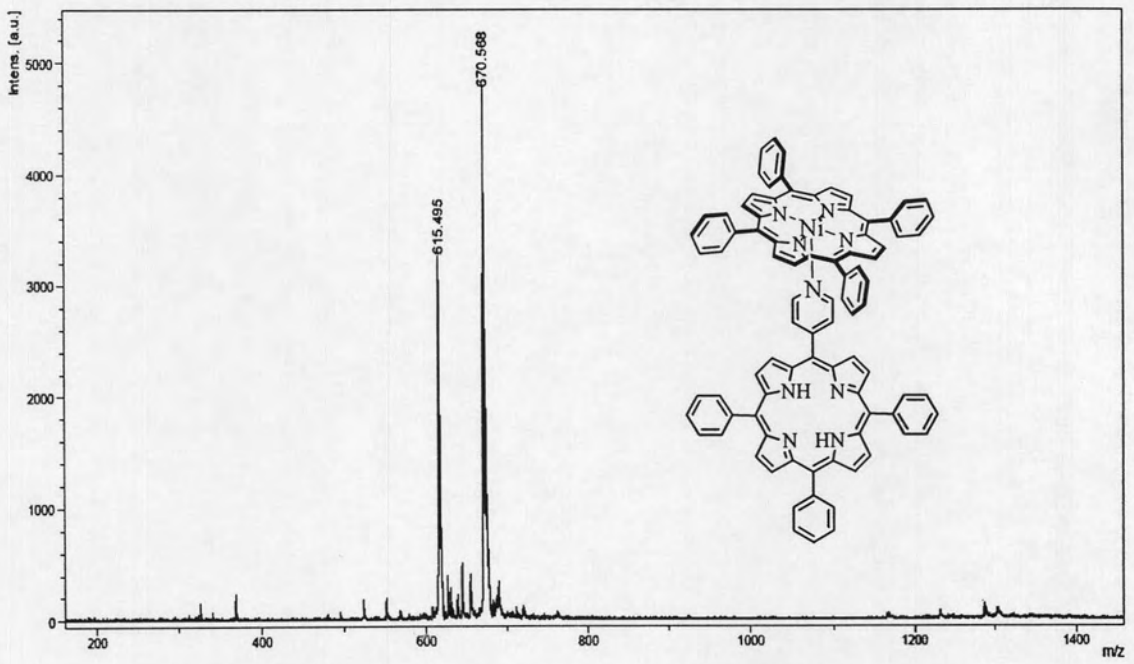

Figure A-71 MALDI-TOF mass spectrum of Ni(TPP)(MPyTPP), (**24**)

APPENDIX B

1. 5,10,15,20-Tetraphenylporphyrin (TPP, 1)

^{1}H NMR ($CDCl_3$, 400 MHz) δ : singlet at -2.73, 2 H_5, signal of internal NH protons
(**Figure A-1**, Appendix A) multiplet at 7. 75-7. 81, 8 H_3 signal of *m*-phenyl protons and 4 H_4 signal of *p*-phenyl protons
multiplet at 8.23-8.25, 8 H_2, signal of *o*-phenyl protons
singlet at 8.88, 8 H_1, signal of β-pyrrole protons

UV/Visible ($CHCl_3$, nm) λ_{max} : 418 (Soret band)
(**Figure A-2**, Appendix A) 516, 550, 592, and 648 (Q bands)

MALDI-TOF MS (dithranol) *m/z* $[M]^+$ Calcd: 614.749; Found: 614.635.
(**Figure A-3**, Appendix A)

2. 5,10,15,20-Tetraphenylporphyrinatozinc(II) (ZnTPP, 2)

^{1}H NMR ($CDCl_3$, 400 MHz) δ : multiplet at 7.75-7.77, 8 H_3 signal of *m*-phenyl
(**Figure A-4**, Appendix A) protons and 4 H_4 signal of *p*-phenyl protons
multiplet at 8.23-8.25, 8 H_2, signal of *o*-phenyl protons
singlet at 8.96, 8 H_1, signal of β-pyrrole protons

UV/Visible ($CHCl_3$, nm) λ_{max} : 423 (Soret band)
(**Figure A-5**, Appendix A) 554 and 598 (Q bands)

MALDI-TOF MS (dithranol) *m/z* $[M]^+$ Calcd: 678.123; Found: 677.492.
(**Figure A-6**, Appendix A)

3. 5,10,15,20-Tetraphenylporphyrinatonickel(II) (NiTPP, 4)

^{1}H NMR ($CDCl_3$, 400 MHz) δ : multiplet at 7.75-7.77, 8 H_3 signal of *m*-phenyl
(**Figure A-10**, Appendix A) protons and 4 H_4 signal of *p*-phenyl protons
multiplet at 8.23-8.25, 8 H_2, signal of *o*-phenyl protons
singlet at 8.96, 8 H_1, signal of β-pyrrole protons

UV/Visible ($CHCl_3$, nm) λ_{max} : 415 (Soret band)
(**Figure A-11**, Appendix A) 528 (Q band)

MALDI-TOF MS (dithranol) *m/z* $[M]^+$ Calcd: 671.426; Found: 671.400.
(**Figure A-12**, Appendix A)

4. 5-(Pyridyl)-10,15,20-triphenylporphyrin (MPyTPP, 8)

^{1}H NMR ($CDCl_3$, 400 MHz) δ : singlet at -2.80, 2 H_9, signal of internal NH protons
(**Figure A-22**, Appendix A) multiplet at 7.81-7.74, 6 H_7 signal of *m*-phenyl protons and 3 H_8 signal of *p*-phenyl protons
multiplet at 8.19-8.17, 2 H_6 signal of 3,5- pyridyl protons
multiplet at 8.23-8.21, 6 H_5 signal of *o*-phenyl protons
doublet at 8.79, 2 H_4, signal of β-pyrrole protons
singlet at 8.87, 4 H_3, signal of β-pyrrole protons
doublet at 8.89, 2 H_2, signal of β-pyrrole protons
doublet at 9.03, 2 H_1, signal of 2,6-pyridyl protons

UV/Visible ($CHCl_3$, nm) λ_{max} : 418 (Soret band)
(**Figure A-23**, Appendix A) 515, 550, 590, and 646 (Q bands)

MALDI-TOF MS (dithranol) *m/z* $[M]^+$ Calcd: 615.737; Found: 615.587.
(**Figure A-24**, Appendix A)

5. 5,15-(Dipyridyl)-10,20-diphenylporphyrin (*trans*-DPyDPP, 9)

^{1}H NMR ($CDCl_3$, 400 MHz) δ : singlet at -2.84, 2 H_8, signal of internal NH protons
(**Figure A-25**, Appendix A) multiplet at 7.76-7.82, 4 H_6, signal of *m*-phenyl protons and 2 H_7 signal of *p*-phenyl protons
multiplet at 8.20-8.22, 4 H_4, signal of *o*-phenyl protons and 4 H_5 signal of 3,5-pyridyl protons
doublet at 8.80, 4 H_3, signal of β-pyrrole protons
doublet at 8.91, 4 H_2, signal of β-pyrrole protons
doublet at 9.05, 4 H_1, signal of 2,6-pyridyl protons

UV/Visible ($CHCl_3$, nm) λ_{max} : 418 (Soret band)
(**Figure A-26**, Appendix A) 515, 549, 590, and 648 (Q bands)

MALDI-TOF MS (dithranol) *m/z* $[M]^+$ Calcd: 616.725; Found: 616.423.
(**Figure A-27**, Appendix A)

6. 5,10-(Dipyridyl)-15,20-diphenyl porphyrin (*cis*-DPyDPP, 10)

^{1}H NMR ($CDCl_3$, 400 MHz) δ : singlet at -2.84, 2 H_{10}, signal of internal NH protons

(**Figure A-28**, Appendix A) multiplet at 7.76-7.82, 4 H_8, signal of *m*-phenyl protons and 2 H_9 signal of *p*-phenyl protons

multiplet at 8.21-8.23, 4 H_6, signal of *o*-phenyl protons and 4 H_7 signal of 3,5-pyridyl protons

doublet at 8.80, 2 H_5, signal of β-pyrrole protons

singlet at 8.85, 2 H_4, signal of β-pyrrole protons

singlet at 8.88, 2 H_3, signal of β-pyrrole protons

doublet at 8.92, 2 H_2, signal of β-pyrrole protons

doublet at 9.05, 4 H_1, signal of 2,6-pyridyl protons

UV/Visible ($CHCl_3$, nm) λ_{max} : 418 (Soret band)

(**Figure A-29**, Appendix A) 515, 549, 590, and 647 (Q band)

MALDI-TOF MS (dithranol) *m/z* $[M]^+$ Calcd: 616.725; Found: 616.508.

(**Figure A-30**, Appendix)

7. 5,10,15-(Tripyridyl)-20-phenylporphyrin (TPyMPP, 11)

^{1}H NMR ($CDCl_3$, 400 MHz) δ : singlet at -2.88, 2 H_9, signal of internal NH protons

(**Figure A-31**, Appendix A) multiplet at 7.76-7.84, 2 H_7, signal of *m*-phenyl protons and 1 H_8 signal of *p*-phenyl protons

multiplet at 8.19-8.21, 2 H_5, signal of *o*-phenyl protons and 6 H_6 signal of 3,5-pyridyl protons

doublet at 8.81, 2 H_4, signal of β-pyrrole protons

singlet at 8.86, 4 H_3, signal of β-pyrrole protons

doublet at 8.92, 2 H_2, signal of β-pyrrole protons

doublet at 9.06, 6 H_1, signal of 2,6-pyridyl protons

UV/Visible ($CHCl_3$, nm) λ_{max} : 417 (Soret band)

(**Figure A-32**, Appendix A) 513, 545, 586, and 648 (Q bands)

MALDI-TOF MS (dithranol) *m/z* $[M]^+$ Calcd: 617.713; Found: 617.401.

(**Figure A-33**, Appendix A)

8. 5-(Pyridyl)-10,15,20-triphenylporphyrinatozinc(II) (ZnMPyTPP, 12)

^{1}H NMR ($CDCl_3$, 400 MHz) δ : multiplet at 7.81, 6 H_7, signal of *m*-phenyl protons
(**Figure A-34**, Appendix A) and 3 H_8 signal of *p*-phenyl protons
multiplet at 8.18-8.21, 6 H_5, signal of *o*-phenyl protons and 2 H_6 signal of 3,5-pyridyl protons
multiplet at 8.77-8.81, 2 H_2, 4 H_3, 2 H_4, signal of β-pyrrole protons
multiplet at 8.97, 2 H_1, signal of 2,6-pyridyl protons

UV/Visible ($CHCl_3$, nm) λ_{max} : 424 (Soret band)
(**Figure A-35**, Appendix A) 555 and 597 (Q bands)

MALDI-TOF MS (dithranol) *m/z* $[M]^+$ Calcd: 679.111; Found: 677.739.
(**Figure A-36**, Appendix A)

9. 5-(Pyridyl)-10,15,20-triphenylporphyrinatonickel(II) (NiMPyTPP, 14)

^{1}H NMR ($CDCl_3$, 400 MHz) δ : multiplet at 8.86, 2 H_2, signal of β-pyrrole protons
(**Figure A-40**, Appendix A) multiplet at 8.77, 4 H_3, signal of β-pyrrole protons
multiplet at 8.64-8.55, 2 H_4 signal of β-pyrrole protons and 2 H_1 signal of 2,6-pyridyl protons
multiplet at 8.01-7.99, 6 H_5 signal of *o*-phenyl protons and 2 H_6 signal of 3,5-pyridyl protons
multiplet at 7.73-7.67, 6 H_7 signal of *m*-phenyl protons and 3 H_8 signal of *p*-phenyl protons

UV/Visible ($CHCl_3$, nm) λ_{max} : 416 (Soret band)
(**Figure A-41**, Appendix A) 529 (Q band)

MALDI-TOF MS (dithranol) *m/z* $[M]^+$ Calcd: 672.414; Found: 670.098.
(**Figure A-42**, Appendix A)

10. 5,10,15,20-Tetrapyridylporphyrin (TPyP, 18)

^{1}H NMR ($CDCl_3$, 400 MHz) δ : multiplet at 9.06, 8 H_1, signal of 2,6-pyridyl protons
(**Figure A-52**, Appendix A) multiplet at 8.87, 8 H_2, signal of β-pyrrole protons
multiplet at 8.16, 8 H_3, signal of 3,5-pyridyl protons
singlet at -2.93, 2 H_4, signal of internal NH protons

UV/Visible ($CHCl_3$, nm) λ_{max} : 418 (Soret band)

(**Figure A-53**, Appendix A) 513, 546, 588, and 644 (Q bands)

MALDI-TOF MS (dithranol) *m/z* $[M]^+$ Calcd: 618.701; Found: 618.577.

(**Figure A-54**, Appendix A)

11. 5,10,15,20-Tetrapyridylporphyrinatozinc(II) (ZnTPyP, 19)

^{1}H NMR (DMSO, 400 MHz) δ : multiplet at 9.02, 8 H_1, signal of 2,6-pyridyl protons

(**Figure A-55**, Appendix A) multiplet at 8.84, 8 H_1, signal of β-pyrrole protons

multiplet at 8.22, 8 H_2, signal of 3,5-pyridyl protons

UV/Visible ($CHCl_3$, nm) λ_{max} : 424 (Soret band)

(**Figure A-56**, Appendix A) 555 and 593 (Q bands)

MALDI-TOF MS (dithranol) *m/z* $[M]^+$ Calcd: 682.076; Found: 680.567.

(**Figure A-57**, Appendix A)

Optical Gas Sensor of 5,10,15,20-tetraphenylporphyrinatozinc(II) (ZnTPP, 2)

The thin film ZnTPP absorption spectrum is signified by the intense Soret band at 433 nm and Q band at 551 nm. The optical absorption spectrum was selectively divided into five intervals, covering the entire range for observable changes, as R1:340-415, R2:415-565, R3:565-625, R4:625-635, and R5:635-795 nm. The alcohol sensing capability of the ZnTPP films has been investigated under dynamic conditions by using a home-built stainless steel chamber with quartz windows for optical measurements. The test was conducted under a flow system at a constant rate of 755 mL/min by using 99.9% nitrogen as both a carrier and a reference gas. The dynamic optical response was monitored by recording the absorbance intensity at fixed interval of 10 min during alcohol exposure and another 10 min during recovery under a nitrogen flow.

The optical absorption response $\Delta A/A_{ZnTPP}$ for each interval was calculated from $(A-A_0)/A_{ZnTPP}$, where A and A_0 are the area integrals measured during alcohol vapor exposure and during the nitrogen gas flow, respectively, and A_{ZnTPP} are the initial area integral of ZnTPP. The typical dynamic responses of alcohol vapor of ZnTPP were similar to what was reported in the literature [54]. The spectral regions of methanol, ethanol, isopropanol, and Thai whisky vapor corresponding to the R3 (565-625 nm) have a positive response, different from the other ranges, which show a negative. The average response ΔS was calculated from the average of $S-S_0$ for all

observable response pulses, where S is the dynamic sensor signal during alcohol vapor exposure and S_0 is the base sensor signal in nitrogen gas flow. The responses of ZnTPP films to alcohols produce the strongest response with Thai whisky in R3 (565-625 nm).

VITA

Mr. Thana Arunwattanachok was born on September 23, 1979 in Bangkok, Thailand. He received a Bachelor degree of Science from Department of Chemistry, Faculty of Science, King Mongkut's University of Technology Thonburi, Thailand in 2002. He worked at Nippon Paint (Thailand) Co, Ltd for 2 years. He was admitted to a Master's Degree Program of Petrochemistry and Polymer Science, Faculty of Science, Chulalongkorn University in 2004 and completed the program in 2006. His address is Ekkachai 45, Ekkachai Road, Bangbon, Bangbon, Bangkok, 10150.